



This is a repository copy of *On the accuracy of nominal, structural, and local stress based approaches in designing aluminium welded joints against fatigue*.

White Rose Research Online URL for this paper:

<https://eprints.whiterose.ac.uk/106901/>

Version: Accepted Version

---

**Article:**

Al Zamzami, I. and Susmel, L. (2017) On the accuracy of nominal, structural, and local stress based approaches in designing aluminium welded joints against fatigue.

International Journal of Fatigue, 101 (Part 2). pp. 137-158. ISSN 0142-1123

<https://doi.org/10.1016/j.ijfatigue.2016.11.002>

---

Article available under the terms of the CC-BY-NC-ND licence  
(<https://creativecommons.org/licenses/by-nc-nd/4.0/>)

**Reuse**

This article is distributed under the terms of the Creative Commons Attribution-NonCommercial-NoDerivs (CC BY-NC-ND) licence. This licence only allows you to download this work and share it with others as long as you credit the authors, but you can't change the article in any way or use it commercially. More information and the full terms of the licence here: <https://creativecommons.org/licenses/>

**Takedown**

If you consider content in White Rose Research Online to be in breach of UK law, please notify us by emailing [eprints@whiterose.ac.uk](mailto:eprints@whiterose.ac.uk) including the URL of the record and the reason for the withdrawal request.



[eprints@whiterose.ac.uk](mailto:eprints@whiterose.ac.uk)  
<https://eprints.whiterose.ac.uk/>

# **On the accuracy of nominal, structural, and local stress based approaches in designing aluminium welded joints against fatigue**

**Ibrahim Al Zamzami and Luca Susmel**

Department of Civil and Structural Engineering, The University of Sheffield,  
Mappin Street, Sheffield S1 3JD, United Kingdom

Corresponding Author: Prof. **Luca Susmel**  
Department of Civil and Structural Engineering  
The University of Sheffield, Mappin Street, Sheffield, S1 3JD, UK  
Telephone: +44 (0) 114 222 5073  
Fax: +44 (0) 114 222 5700  
E-mail: [l.susmel@sheffield.ac.uk](mailto:l.susmel@sheffield.ac.uk)

## **ABSTRACT**

This paper investigates the accuracy and reliability of nominal stresses, hot-spot stresses, effective notch stresses, notch-stress intensity factors (N-SIFs) and material length scale parameters in estimating fatigue lifetime of aluminium welded joints. This comparative assessment was based on a large number of experimental data taken from the literature and generated by testing, under either cyclic axial loading or cyclic bending, a variety of aluminium welded structural details. Whenever it was required, stress analyses were performed by solving bi-dimensional linear-elastic finite element models. The obtained results demonstrate that the effective notch stress method, the N-SIF approach, and the Theory of Critical Distances (TCD) provide a more accurate fatigue life estimation in comparison with the other methodologies. In this context, the TCD was seen to be easier to adopt, requiring less computational effort than the effective notch stress method and the N-SIF approach. Finally, based on the experimental results being re-analysed, a unifying value of 0.5 mm is proposed for the TCD critical distance, with this value allowing aluminium welded connections to be designed accurately irrespective of joint geometry's complexity.

**Keywords:** welded joints, aluminium, nominal stress, local stress, mean stress, critical distance, design fatigue curves

## Nomenclature

$c_0, c_1$	constants in the linear regression function
$f(R)$	mean stress enhancement factor
$k$	negative inverse slope
$k_I$	non-dimensional parameter to estimate $K_I$ and $\Delta K_I$
$K_I, K_{II}$	notch-stress intensity factor (N-SIF) for Mode I and Mode II loading
$L$	thickness of secondary attachment
$L_{W-Al}$	critical distance for aluminium welded joints
$n$	number of experimental data
$N_A$	reference number of cycles to failure
$N_f$	number of cycles to failure
$P$	proportion of the distribution
$P_S$	probability of survival
$q$	factor for one-sided tolerance limits for normal distribution
$r, \theta$	polar coordinates
$r_n$	notch root radius
$r_{ref}$	reference radius
$R$	load ratio ( $R = \sigma_{min} / \sigma_{max}$ )
$t$	thickness
$T_\sigma$	scatter ratio of the endurance limit range for $P_S = 90\%$ and $P_S = 10\%$
$z$	weld leg length
$\Delta K_I$	mode I N-SIF range
$\Delta K_{I,50\%}$	mode I N-SIF range extrapolated at $N_A$ cycles to failure for $P_S = 50\%$
$\Delta K_{I,97.7\%}$	mode I N-SIF range extrapolated at $N_A$ cycles to failure for $P_S = 97.7\%$
$\Delta \sigma$	stress range
$\Delta \sigma_{0.4t}$	range of the superficial stress at a distance from the weld toe equal to $0.4 \cdot t$
$\Delta \sigma_t$	range of the superficial stress at a distance from the weld toe equal to $t$
$\Delta \sigma_1$	range of the maximum principal stress
$\Delta \sigma_{A,50\%}$	endurance limit range at $N_A$ cycles to failure for $P_S = 50\%$
$\Delta \sigma_{A,95\%}$	endurance limit range at $N_A$ cycles to failure for $P_S = 95\%$
$\Delta \sigma_{A,97.7\%}$	endurance limit range at $N_A$ cycles to failure for $P_S = 97.7\%$
$\Delta \sigma_{HS}$	hot-spot stress range
$\Delta \sigma_{nom}$	nominal stress range
$\Delta \sigma_{NS}$	notch stress range
$\Delta \sigma_{PM}$	range of the Point Method local stress
$\lambda_1, \lambda_2, \chi_1, \chi_2$	constants in William's equations
$\sigma_{max}$	maximum stress in the cycle
$\sigma_{min}$	minimum stress in the cycle
$\sigma_\theta, \sigma_r$	linear-elastic local normal stresses
$\tau_{r\theta}$	linear-elastic local shear stress

## 1. Introduction

Welding processes induce residual stresses, defects, imperfections, distortions, etc. that strongly affect the fatigue strength of welded details [1-3]. Further, both weld seams and weld roots act as stress concentrators resulting in severe local stress/strain gradients. In this context, performing the fatigue assessment of welded connections is a complex problem that must be addressed properly in order to avoid unwanted in-service failures. To this end,

structural engineers need reliable approaches that not only are accurate and reliable, but also allow the time and costs associated with the design process to be minimised [4].

In recent years, using aluminium as a structural material has become an interesting alternative solution in important applications such as automotive frames, offshore structures and also in the railway industry. The reason behind this growth is the ability to utilise the various mechanical/physical properties of aluminium alloys to manufacture high-performance lightweight structures having increased strength-to-weight ratio. Further, aluminium is a “green” material that can efficiently be recycled *ad infinitum*.

In spite of the important role played by aluminium in structural engineering applications, examination of the state of the art shows that, compared to welded steel, less theoretical and experimental effort has been made so far in order to model and assess the fatigue behaviour of welded aluminium effectively.

The available Standards and Codes of Practise take as a starting point the assumption that welded aluminium alloys have the same fatigue strength regardless their chemical composition. Although this assumption results in a great simplification of the design problem, it increases the level of uncertainty associated with fatigue assessment process [5]. These design uncertainties lead to components and structures that are bigger and heavier than necessary, with this resulting in an inefficient usage of materials and energy during manufacturing.

In this investigation, the accuracy of design approaches based on nominal stresses, hot-spot stresses, effective notch stresses, notch stress intensity factors (N-SIFs) and the Theory of Critical Distance (TCD) was assessed systematically against a large number of experimental results taken from the technical literature. The selected data were generated by testing aluminium welded joints under either cyclic axial loading or cyclic bending. The geometries of the structural details being investigated are shown in Figure 1a. Furthermore, owing to the important role played by the presence of superimposed static stress, also the influence of non-zero mean stresses on aluminium welded joints' overall fatigue strength was investigated in detail.

The global stress method (also known as the nominal stress method) is the most simple and widely used approach to design weldments against fatigue [6-8]. When either nominal stresses cannot be calculated unambiguously or a reference fatigue curve for the specific geometry of the welded detail being assessed is not available, then either hot-spot or local stress based approaches are recommended to be used [9-12].

The structural hot-spot stress method is applied by determining, on the component surface, the linear-elastic stress states at either two or three reference points. Subsequently, by using these reference stress states, structural stresses are extrapolated to the weld toes at the hot spots [6]. Structural stresses can be determined experimentally by using strain gauges attached to the component's surface at different distances from the weld toe. Obviously, this experimental procedure is not applicable when the area of interest in the vicinity of the weld is not accessible (for instance, hidden details) [6, 12]. This problem can be overcome by estimating the stress states at the extrapolation points via linear-elastic Finite Element (FE) models. The hot-spot method was originally developed to assess the fatigue behaviour of offshore structures, with its use being subsequently extended to other structural applications [10, 11].

Since the beginning of the 1990s, a number of advanced local stress based approaches has been developed and validated with the aim of improving the accuracy in estimating fatigue lifetime of welded connections. In this context, certainly the effective notch stress method, the N-SIF approach, and the TCD deserve to be mentioned explicitly.

The effective notch stress approach makes use of linear-elastic stresses determined at either the weld toe or the weld root by introducing a fictitious fillet having radius equal to 1 mm, with this strategy being applicable to welded joints having thickness larger than (or equal to) 5 mm. On the contrary, when the relevant thickness is lower than 5 mm, the effective notch stress approach is recommended as being applied by using a fictitious radius of 0.05 mm [6, 12-13]. This approach can be used to assess welded joint in which the fatigue crack initiation process takes place not only at weld toes, but also at weld roots.

At the end of the 1990s, by taking full advantage of William's analytical solution [14], Tovo and Lazzarin formulated the so-called N-SIF approach [15, 16]. As far as failures at the weld toes are concerned, the N-SIF approach estimates fatigue lifetime of welded components by modelling the weld seams as V-notches having opening angle equal to  $135^\circ$  and root radius equal zero [15-18]. The N-SIF approach can also be used to perform the fatigue assessment of welded joints in which cracks initiate at the weld roots, provided that a specific reference design curve is employed [16].

The TCD [19, 20] assesses the fatigue strength of welded joints by post-processing the relevant linear-elastic local stress fields via a material characteristic length that is directly related to the size of the dominant source of microstructural heterogeneity. According to the TCD's *modus operandi*, this critical distance is treated as a material property whose value is independent from type of applied loading, geometry, notch profile, and size of the component being assessed [5, 19-21].

In the complex scenario depicted above, the goal of the present investigation is to check the accuracy of the aforementioned fatigue design methods in estimating fatigue lifetime of aluminium welded joints against a large number of data taken from the literature. To use both the hot-spot approach and the considered local stress methods to post-process the experimental data being selected, a number of linear-elastic FE models was solved using commercial FE code ANSYS®. The N-SIF approach was applied also by using the formulas derived by Lazzarin and Tovo by post-processing the results from a large number of linear-elastic FE models, with these formulas allowing the N-SIF range,  $\Delta K_I$ , to be estimated directly for standard welded geometries [16, 17, 22, 23]. Finally, the N-SIF master curve proposed by Lazzarin and Livieri [17, 21, 22] was used to determine a unifying value for the TCD critical distance suitable for accurately estimating the fatigue lifetime of aluminium welded joints.

## 2. Data base, statistical re-analysis, and reference fatigue curves

To assess the accuracy of the considered design methods in estimating fatigue lifetime of aluminium welded joints, more than two thousand experimental results were selected from the technical literature [24-45]. These data were generated by testing, under either cyclic axial loading or cyclic bending, a variety of welded specimens (Fig. 1a) made of different aluminium alloys.

The specimens considered in the present investigation were tested under load ratios,  $R = \sigma_{\min} / \sigma_{\max}$ , ranging from -1 up to 0.75.

According to the design strategies suggested both by Eurocode 9 (EC9) [46] and by the International Institute of Welding (IIW) [6, 9], initially the experimental results being considered were post-processed in terms of stress ranges by disregarding the presence of superimposed static stress. Subsequently, the same data were re-analysed in order to investigate explicitly the effect of non-zero mean stresses on the fatigue behaviour of aluminium welded joints (Section 8).

Figure 1a summarises the different types of welded specimens that were assessed according to the nominal stress approach. The hot-spot method and the considered local stress approaches were applied solely to series Ba, Bb, Ca and Cb (Fig. 1a). This is due to the fact that, for the other series, the relevant local dimensions of the welds were not reported in the original sources.

For a given definition of the design stress range, the data sets being investigated were post-process to obtain the corresponding fatigue curves. These curves were determined by re-analysing the fatigue results under the hypothesis of a log-normal distribution of the number of cycles to failure,  $N_f$ , for each stress level, with the confidence level being taken equal to 95% [47, 48]. The mathematical procedure followed to post-process the considered experimental data is summarised in Appendix A. According to this standard procedure, in what follows the results from the statistical re-analyses will be reported in terms of (see Fig. 1b): negative inverse slope,  $k$ , range of the endurance limit,  $\Delta\sigma_{A,97.7\%}$ , extrapolated at  $2 \cdot 10^6$  cycles to failure for a Probability of Survival,  $P_s$ , equal to 97.7%, and scatter ratio of the

endurance limit range for 90% and 10% probabilities of survival,  $T_\sigma$  (i.e.,  $T_\sigma = \Delta\sigma_{10\%} / \Delta\sigma_{90\%}$ ). Ratio  $T_\sigma$  is a useful index allowing the level of scattering associated with a population of fatigue data to be quantified. As to the recommended values for  $T_\sigma$ , Haibach [49] has demonstrated that, on average, the series of fatigue data generated by testing steel welded joints are characterised by a  $T_\sigma$  ratio equal to 1.5. This reference value was derived by post-processing a large number of experimental results from different welded structural details made of steel [49].

For what concerns the nominal stress approach, the required reference design curves were taken from EC9 [49] as well as from the IIW Recommendations [6]. The accuracy of the estimates obtained by applying both the hot-spot stress approach and the effective notch stress approach were compared with the reference curves supplied by the IIW [6].

It is worth recalling here that the EC9 design curves refer to  $P_S=97.7\%$ , whereas those reported in the IIW Recommendations to  $P_S=95\%$ . The values for the endurance limits suggested both by EC9 and the IIW are extrapolated at  $2 \cdot 10^6$  cycles to failure. The IIW recommends a constant negative inverse slope,  $k$ , equal to 3, whilst EC9 supplies different negative inverse slopes for different welded geometries.

Finally, Lazzarin and Livieri's master curve for aluminium welded joints [17, 22, 23] was used to assess the predictions made according to the N-SIF approach.

### **3. Fatigue assessment using the Nominal Stress based approach**

As far as the nominal stress approach is concerned, design stresses are calculated using the classic continuum mechanics concepts. In particular, nominal stresses have to be determined by explicitly taking into account those stress gradients resulting from the macro-geometrical features characterising the welds regions [1, 50]. On the contrary, the stress concentration phenomena arising from the weld toes have to be disregarded, since the effect of the local stress gradients is already included in the fatigue strength values supplied by both EC9 and the IIW. Accordingly, the selection of an appropriate design curve is essential to achieve accurate fatigue design [6, 51].

Tables 1 to 6 summarise the results obtained by using the nominal stress approach to post-process, according to the statistical procedure reviewed in Appendix A, the individual data sets being investigated. Endurance limit ranges  $\Delta\sigma_{A,50\%}$  and  $\Delta\sigma_{A,97.7\%}$  reported in Tables 1 to 6 were extrapolated at  $2 \cdot 10^6$  cycles to failure for  $P_s$  equal to 50% and 97.7%, respectively.

These tables show that, on average, the negative inverse slope of the fatigue curves determined from the individual series is larger than the values that are recommended both by EC9 and by the IIW. Another important aspect is that, according to Tables 1 to 6, the average value of  $T_\sigma$  is equal to 2.2 with a standard deviation of 1.3. This suggests that, as far as aluminium welded joints are concerned, the expected value for  $T_\sigma$  is larger than the reference value of 1.5 that is suggested by Haibach for steel weldments [49].

The experimental results listed in Tables 1 to 6 are also summarised in the Wöhler diagrams reported in Figure 2. In more detail, these log-log charts plot the range of the nominal stress,  $\Delta\sigma_{nom}$ , vs. the number of cycles to failure,  $N_f$ , for the different structural details being considered (Fig. 1a). For each welded geometry, the fatigue curves suggested by EC9 (grey continuous line) and the IIW (black continuous line) are also plotted in Figure 2 to allow the experimental results to be contrasted with the standard/recommended design guidelines.

The fatigue curves for  $P_s=50\%$  and  $P_s=97.7\%$  determined, according to the statistical procedure reviewed in Appendix A, by post-processing all the experimental results generated by testing the same type of structural detail are summarised in Table 7. In this table, the obtained values are directly compared to the corresponding design curves in terms of negative inverse slope and endurance limit range extrapolated at  $2 \cdot 10^6$  cycles to failure.

Figure 2 shows that, in general, the design curves recommended by EC9 result in more conservative estimates than those obtained by using the IIW design curves. Further, these Wöhler diagrams together with Table 7 demonstrate that, for a given welded geometry, the negative inverse slope calculated from the entire population of data is lower than the corresponding value suggested by both EC9 and the IIW. This is an interesting aspect, especially in light of the fact that, as shown in Tables 1 to 6, the negative inverse slope of the individual data sets is, in general, larger than the corresponding standard value.

Finally, it is important to highlight that the use of the design curves recommended both by EC9 and by the IIW to assess butt (Ab) and load-carrying cruciform (Ca) welded joints is seen to result in estimates that are slightly non-conservative.

#### **4. Fatigue assessment using the Hot-Spot Stress approach**

The Hot-Spot Stress approach takes as its starting point the idea that the gradient characterising the stress field distribution in the vicinity of the weld toe can be modelled effectively via the linear-elastic stress states determined at two or three reference superficial points positioned at given distances from the weld toe itself [52]. Subsequently, via these reference stress states, structural stresses are extrapolated to the weld toes at the hot spots (Fig. 3a). By so doing, the effects of the local stress gradients can be taken into account indirectly via specific reference fatigue curves [6, 53].

In situations of practical interest, the Hot-Spot Stress approach is applied by determining the required reference stresses using strain gauges and/or solving linear-elastic FE models. In the latter case, hot-spot stresses can be estimated either via surface stress extrapolation or via through thickness stress linearization [6, 53]. Another interesting method is the one proposed by Dong which is based on the linearized equilibrium of the normal and shear stresses acting on the weld toe region where the effect of the local stress singularities can be neglected with little loss of accuracy [54].

In the present investigation, hot-spot stresses were determined numerically according to the IIW procedure which is based on the use of different reference distances, with these lengths depending on type of hot-spot stress and quality of mesh [6]. Linear-elastic bi-dimensional FE models were solved via commercial software ANSYS®. Weld beads were modelled as sharp V-notches, i.e., by taking the fillet radius along the intersection line between weld and parent material invariably equal to zero. The models were meshed according to the rules recommended by the IIW via eight-noded solid quadratic elements (Plane 183). The mesh density was varied throughout the welded details in order to obtain in the vicinity of the weld toes finely meshed regions with element size in the range 0.2-0.3 mm (Fig. 4a). Parent and

filler aluminium alloys were treated as linear-elastic, isotropic and homogenous materials with Young's modulus equal to 68 GPa and Poisson's ratio equal to 0.33 [19]. Via these FE models, the corresponding hot-spot stresses were calculated using the surface stress extrapolation method as shown in Figure 3a. In particular, normal stresses were determined at two reference points positioned at a distance from the weld toe equal to  $0.4 \cdot t$  and  $t$ , respectively, with  $t$  being the thickness of the main plate as defined in Figure 1a [6].

The results from the statistical re-analysis performed by post-processing structural welded details Ba, Bb, Ca and Cb (Fig. 1a) according to the Hot-Spot Stress approach are summarised in Tables 8 to 11. The same data are also plotted in the Wöhler diagrams reported in Figure 3b. The values of both the negative inverse slope,  $k$ , and the endurance limit range ( $\Delta\sigma_{A,50\%}$  and  $\Delta\sigma_{A,97.7\%}$ ) at  $2 \cdot 10^6$  cycles to failure that were determined by re-analysing, for any given welded geometry, the entire population of data are reported in Table 7.

The Wöhler diagrams of Figure 3b demonstrate that, as long as non-load-carrying cruciform connections (Ba) and T-joints (Bb) are concerned, the use of the hot-spot approach together with the design fatigue curves supplied by the IIW resulted in estimates that are not only accurate, but also characterised by an adequate level of conservatism. On the contrary, the use of the IIW design curves returned estimates that are characterised by a certain degree of non-conservatism when they are employed to assess the strength of load-carrying fillet welded joints (series Ca and Cb in Figure 1a). As to this aspect, it is interesting to observe that for these welded geometries the level of non-conservatism is seen to increase as the load ratio increases.

To conclude, according to both Figure 3b and Table 7, it can be noted that, for a given type of structural detail, the negative inverse slopes determined by reanalysing the entire population of data are lower not only than the  $k$  values associated with the individual data sets (Tables 8 to 11), but also than the unifying value of 3 recommended by the IIW.

## 5. Fatigue assessment using the Effective Notch Stress approach

The effective notch stress approach is the most advanced fatigue design methodology recommended by the IIW. This method is based on the assumption that fatigue strength can be estimated accurately by using linear-elastic notch stresses determined by rounding either the weld toes or at the weld roots [53, 55, 56] (Fig. 6a). By taking advantage of the micro-support theory proposed by Neuber to model sharp cracks, back in the 1980s Radaj [57-61] has proposed to use a fictitious weld toe/root radius,  $r_{ref}$ , of 1 mm to assess the fatigue strength of welded connections having thickness larger than (or equal to) 5 mm. In contrast, for thin welded details having thickness lower than 5 mm, a fictitious radius,  $r_{ref}$ , of 0.05 mm is recommended as being employed [12, 13, 50, 57]. The notch stress approach is restricted to welded joints in which fatigue cracks initiate either at the weld toe or at the weld root and, under uniaxial fatigue loading, the required stress analyses have to be performed in terms of maximum principal stress range.

As far as thick aluminium welded joints (i.e.,  $t \geq 5$  mm) are concerned, the IIW suggests performing the fatigue assessment via a master design curve characterised by an inverse negative slope equal to 3 and a notch stress endurance limit range,  $\Delta\sigma_{A,97.7\%}$ , at  $2 \cdot 10^6$  cycles to failure equal to 71 MPa (for  $P_S=97.7\%$ ). Turning to aluminium welded joints having thickness lower than 5 mm, as mentioned earlier, weld toes and roots are recommended to be rounded by adopting a fictitious radius of 0.05 mm. To design thin aluminium welded joints against fatigue, Sonsino [55] suggests employing a reference design curve having inverse negative slope equal to 3 and notch stress endurance limit range,  $\Delta\sigma_{A,97.7\%}$ , at  $2 \cdot 10^6$  cycles to failure equal to 180 MPa (for  $P_S=97.7\%$ ).

The collected data were re-analysed by using FE code ANSYS® to solve linear-elastic bi-dimensional models. In these models, the same element type and the same material properties as those used to calculate hot-spot stresses were employed. According to the thickness value, the structural details being investigated were modelled by rounding the toes/roots with a circular fillet having radius equal to either 1 mm or 0.05 mm, this depending on the actual thickness of the main plate. As recommended by the IIW, the mesh

in the vicinity of the fictitious fillets was refined until convergence occurred (Fig 4b). This refinement process led to elements having size in the critical regions ranging between 0.04-0.06 mm for  $r_{ref}=1$  mm and between 0.0025-0.0035 mm for  $r_{ref}=0.05$  mm.

The results from the statistical re-analysis performed by post-processing welded geometries Ba, Bb, Ca and Cb (Fig. 1a) in terms of linear-elastic notch stress are listed in Tables 8 to 11. The individual experimental results are plotted instead in the log-log charts of Figure 5b. Table 7 lists the values of  $k$  as well as of  $\Delta\sigma_{A,50\%}$  and  $\Delta\sigma_{A,97.7\%}$  at  $2 \cdot 10^6$  cycles to failure determined by re-analysing the entire population of data for any welded geometry being considered.

The Wöhler diagrams of Figure 5b show that the use of the Effective Notch Stress approach along with the design fatigue curve supplied by the IIW [6] for  $t \geq 5$  mm and by Sonsino [55] for  $t < 5$  mm resulted in estimates that are not only accurate, but also characterised by an adequate level of conservatism.

To conclude, according to both Figure 5b and Table 7, although the in-field usage of this approach requires a considerable computational effort, the Effective Notch Stress approach certainly is the most accurate design method amongst those recommended by the IIW.

## 6. Fatigue assessment using N-SIF approach

According to Williams [14], linear-elastic stress fields in the vicinity of V-notches with root radius,  $r_n$ , equal to zero can be written as follows for Mode I and Mode II loading, respectively [15] (Fig. 6a):

$$\left\{ \begin{array}{l} \sigma_\theta \\ \sigma_r \\ \tau_{r\theta} \end{array} \right\}_{r_n=0} = \frac{1}{\sqrt{2\pi}} \frac{r^{\lambda_1-1} K_I}{(1+\lambda_1) + \chi_1(1-\lambda_1)} \cdot \left[ \left\{ \begin{array}{l} (1+\lambda_1)\cos(1-\lambda_1)\theta \\ (3-\lambda_1)\cos(1-\lambda_1)\theta \\ (1-\lambda_1)\sin(1-\lambda_1)\theta \end{array} \right\} + \chi_1(1-\lambda_1) \left\{ \begin{array}{l} \cos(1+\lambda_1)\theta \\ -\cos(1+\lambda_1)\theta \\ \sin(1+\lambda_1)\theta \end{array} \right\} \right] \quad (1)$$

$$\left\{ \begin{array}{l} \sigma_\theta \\ \sigma_r \\ \tau_{r\theta} \end{array} \right\}_{r_n=0} = \frac{1}{\sqrt{2\pi}} \frac{r^{\lambda_2-1} K_{II}}{(1-\lambda_2) + \chi_2(1+\lambda_2)} \cdot \left[ \left\{ \begin{array}{l} -(1+\lambda_2)\sin(1-\lambda_2)\theta \\ -(3-\lambda_2)\sin(1-\lambda_2)\theta \\ (1-\lambda_2)\cos(1-\lambda_2)\theta \end{array} \right\} + \chi_2(1+\lambda_2) \left\{ \begin{array}{l} -\sin(1+\lambda_2)\theta \\ \sin(1+\lambda_2)\theta \\ \cos(1+\lambda_2)\theta \end{array} \right\} \right] \quad (2)$$

where  $\lambda_i$  and  $\chi_i$  ( $i=1, 2$ ) are parameters that depend on the opening angle of the V-notch being assessed [15, 62].  $K_I$  and  $K_{II}$  are the N-SIFs for Mode I and Mode II loading, respectively, and are defined as follows:

$$K_I = \sqrt{2\pi} \lim_{r \rightarrow 0} \left[ (\sigma_\theta)_{\theta=0} r^{1-\lambda_1} \right] \quad (3)$$

$$K_{II} = \sqrt{2\pi} \lim_{r \rightarrow 0} \left[ (\tau_{\theta r})_{\theta=0} r^{1-\lambda_2} \right] \quad (4)$$

The N-SIF approach was first proposed by Verreman and Nie [63] back in the mid-1990s. This approach takes as a starting point the fact that [64, 65], according to Eqs (1) and (2), linear-elastic stress fields in the vicinity of sharp V-notches can be described concisely by using N-SIFs. Accordingly, Verreman and Nie argued that this stress parameters could be employed directly to model the crack-initiation process in fillet welded joints subjected to fatigue loading [63]. A couple of years later, this approach was further developed by Tovo and Lazzarin who devised a more rigorous theoretical framework by proposing a formal definition for the N-SIFs [15]. In particular, they observed that in fillet welded joints under nominal axial loading the contribution due to the Mode II stress components can be neglected with little loss of accuracy. This is a consequence of the fact that Mode II stresses are no longer singular for opening angles larger than about  $100^\circ$  [15, 62]. The accuracy and reliability of the N-SIF approach was initially checked by considering steel fillet welded joints with thickness varying in the range 13-100 mm. Subsequently, Lazzarin and Livieri extended the use of this design method to aluminium welded joints by proposing a specific design curve that was derived by considering a large number of experimental data [22]. This master curve is characterised by a reference Mode I N-SIF range,  $\Delta K_{I,97.7\%}$ , at  $5 \cdot 10^6$  cycles to failure equal to  $74 \text{ MPa} \cdot \text{mm}^{0.326}$  (for  $P_s=97.7\%$ ) and a negative inverse slope equal to 4.

In the present investigation, to re-analyse the experimental data generated by testing non-load carrying fillet welded joints, Mode I N-SIF ranges were estimated using the following relationship [15, 16]:

$$\Delta K_I = k_I \cdot \Delta \sigma_{nom} \cdot t^{1-\lambda_1} \quad (5)$$

where  $k_I$  is a non-dimensional parameter which depends on the absolute dimensions of the joint,  $\Delta \sigma_{nom}$  is the range of the nominal stress, and  $t$  is the thickness of the main plate.

The Mode I N-SIF ranges associated with the other geometries were instead determined numerically according to definition (3). In the solved FE models, fillet welds were modelled by setting the toe radius equal to zero. The mesh density in the weld region (Fig. 4c) and the associated N-SIF values were then determined according to the numerical procedure proposed by Tovo and Lazzarin in Ref. [15, 16].

The results from the statistical re-analysis performed by post-processing welded geometries Ba, Bb, Ca and Cb (Fig. 1a) according to the N-SIF approach are listed in Tables 8 to 11. The corresponding individual experimental data are instead plotted in the  $\Delta K_I$  vs.  $N_f$  diagrams reported in Figure 6b. The values of both the negative inverse slope,  $k$ , and the endurance limits expressed in terms of N-SIF range extrapolated at  $2 \cdot 10^6$  cycles to failure (i.e.,  $\Delta K_{I,50\%}$  for  $P_s=50\%$  and  $\Delta K_{I,97.7\%}$  for  $P_s=97.7\%$ ) that were determined by re-analysing, for any given welded geometry, the entire population of data are reported in Table 7.

According to the charts of Figure 6b, Lazzarin and Livieri's master curve was capable of estimating the considered experimental results with a high level of accuracy, with this holding true independently of the type of joint being considered. It is interesting to observe that, as for the approaches investigated in the previous sections, the level of conservatism characterising the N-SIF approach is seen to decrease as the applied load ratio increases. Nevertheless, the diagrams of Figure 6b further confirm that the N-SIF approach is a

powerful design tool suitable for designing aluminium welded joint against fatigue by systematically reaching an adequate level of accuracy/safety.

## **7. Fatigue assessment using the TCD**

As far as notched components are concerned, the TCD assesses the detrimental effect of stress gradients by post-processing the entire linear-elastic stress fields acting on the material in the vicinity of the assumed crack initiation locations [19, 20]. The key feature of this theory is that the required design stress is determined via a specific length scale parameter that takes into account the microstructural features of the material being assessed. The TCD can be formalised in different ways that include the Point Method (PM), Line Method (LM), Area Method (AM), and Volume Method (VM) [5, 20]. The PM and the LM were first introduced in about the mid of the last century by Peterson [66] and Neuber [67], respectively, to perform the high-cycle fatigue assessment of notched metallic materials. In these formalisations of the TCD, the required critical distances were determined empirically by post-processing a large number of experimental results. Subsequently, in the 1980s-1990s Tanaka [68] and Taylor [19] provided a simple way to estimate the critical distance value, with this well-known formula being based on the combined use of the Linear Elastic Fracture Mechanics mechanical properties and the plain material fatigue strength.

The PM represents the simplest formalisation of the TCD and postulates that the stress to be used to estimate the fatigue damage extent is equal to the linear elastic-stress determined at a given distance from the assumed crack initiation location. Its simplicity makes the PM a straightforward design tool suitable for being used in situations of practical interest to perform the fatigue assessment of real welded components. Accordingly, in the present investigation the accuracy of the TCD in estimating fatigue lifetime of aluminium welded joints was checked by applying this powerful theory solely in the form of the PM.

Following a strategy similar to the one adopted in Ref. [5], the PM was calibrated by making the following assumptions:

- the fatigue strength of ground butt welded joints under uniaxial fatigue loading is modelled via the EC9 fatigue curve recalculated for  $P_S=50\%$  (i.e.,  $\Delta\sigma_{A,50\%}=79.2\text{MPa}$  at  $2\cdot 10^6$  cycles to failure and  $k=4.5$ );
- the  $P_S=50\%$  reference master curve suggested by Lazzarin and Livieri for aluminium welded joints ( $\Delta K_{I,50\%}=124.5\text{ MPa}\cdot\text{mm}^{0.326}$  at  $2\cdot 10^6$  cycles to failure and  $k=4$  [22]) is used as reference notch fatigue curve.

By using these two pieces of calibration information, a unifying value for the critical distance,  $L_{W-Al}$ , suitable for designing aluminium welded joints was then determined as follows:

- by making  $t$ ,  $L$  and  $z$  vary (see welded geometry Ca in Figure 1a), the  $P_S=50\%$  N-SIF master curve and Eq. (5) were used to estimate the corresponding nominal stress range,  $\Delta\sigma_{nom,50\%}$ , at  $2\cdot 10^6$  cycles to failure;
- subsequently, under the estimated values for  $\Delta\sigma_{nom,50\%}$ , the corresponding local stress distributions were determined along the weld toe bisector in terms of maximum principal stress  $\Delta\sigma_1$  (Fig. 6a) [4, 5], with these stress-distance curves being estimated both numerically (Fig. 4c) and analytically via Eq. (1);
- finally, according to the PM, by plotting, at  $2\cdot 10^6$  cycles to failure, the linear-elastic stress field for the welded geometry being considered as well as the ground butt weld endurance limit, i.e.,  $\Delta\sigma_{A,50\%}=79.2\text{ MPa}$ , critical distance value  $L_{W-Al}$  was estimated directly via the abscissa of the point at which these two stress-distance curves crossed each other (Fig. 6a).

Since Lazzarin and Livieri's N-SIF master curve was determined by post-processing a large number of experimental data generated by testing aluminium cruciform joints having absolute dimensions in the range 3-24mm [22, 23], the procedure describe above was

applied by considering different values for  $t$ ,  $L$  and  $z$  (see welded geometry Ca in Figure 1a). This was done in order to check whether the estimated critical distances were affected by the absolute dimensions of the welded joint being used for calibration (scale effect in fatigue). Table 12 summarises the results of this sensitivity analysis that was performed by taking  $t$ ,  $L$  and  $z$  equal to 8, 12, 16 and 20mm. Table 12 demonstrates that, from an engineering point of view, the influence of the welded connection's absolute dimensions on the estimated values for length  $L_{W-Al}$  can be neglected with little loss of accuracy. Accordingly, for the sake of design simplicity, the  $L_{W-Al}/2$  value to apply the PM to design aluminium welded joints against fatigue was taken invariably equal to 0.25 mm, i.e.:

$$L_{W-Al} = 0.5 \text{ mm} \tag{6}$$

Once the critical distance was determined, the experimental results summarised in Tables 8 to 11 were post-processed to determine the linear-elastic PM stress range,  $\Delta\sigma_{PM}$ , at a distance from the weld toe equal to  $L_{W-Al}/2=0.25$  mm (Fig. 6a), the required linear-elastic stress fields being determined by taking the weld toe radius invariably equal to zero. The experimental results summarised in the above tables are also plotted in the  $\Delta\sigma_{PM}$  vs.  $N_f$  log-log diagrams reported in Figure 6b, the  $P_S=97.7\%$  reference design curve being that recommended by EC9 to assess the fatigue strength of ground butt welded joints (i.e.,  $\Delta\sigma_{A,97.7\%}=55$  MPa at  $2\cdot 10^6$  cycles to failure and  $k=4.5$ ). These charts make it evident that the TCD applied by taking  $L_{W-Al}/2=0.25$  mm resulted in highly accurate estimates, with this holding true independently of type of joint and absolute dimensions. It is also interesting to observe that, according to Table 7, the negative inverse slope,  $k$ , determined, for any considered welded geometry, by post-processing the entire population of data was seen to be lower than the value of 4.5 characterising the EC9 design curve used as reference information not only to estimate  $L_{W-Al}$ , but also to assess the overall accuracy of the PM (Fig. 6b). This results in the fact that, as for the other design methods being considered in the present investigation, the endurance limits

for series Ba, Bb, Ca and Cb were seen to be lower than the corresponding endurance limit of the EC9 reference design fatigue curve being adopted (see Table 7).

To conclude, the charts of Figure 6b fully support the idea that the TCD can be used to perform the fatigue assessment of aluminium weldments by directly post-processing the linear-elastic stress fields acting on the material in the weld regions. Its systematic usage was seen to result in highly accurate estimates, the computational effort required for its in-field usage being lower than the one required to apply both the Effective Notch Stress method and the N-SIF approach.

## **8. Effect of non-zero mean stresses on the fatigue strength of aluminium weldments**

Independent of the definition being adopted to determine the required design stress, much experimental evidence suggests that, as far as welded connections are concerned, the presence of superimposed static stresses plays a minor role in the overall fatigue strength of welded joints [53]. This is a consequence of the fact that the residual stresses arising from the welding process alter the actual value of the load ratio in the vicinity of the crack initiation locations. Therefore, in the presence of high tensile residual stresses, the local value of  $R$  is seen to be different from the nominal load ratio characterising the load history under investigation, with the local  $R$  ratio becoming larger than zero also under fully-reversed nominal fatigue loading. Accordingly, connections in the as-welded condition are usually assessed via reference design curves that are determined experimentally under  $R > 0$ . Whilst the above simplification is seen to result in reasonable fatigue life predictions for steel welded joints, unfortunately, it does not always return satisfactory results with aluminium weldments. This is due to the fact that nominal load ratios lower than zero can affect the fatigue behaviour not only of stress relieved, but also of as-welded aluminium joints [12]. Accordingly, under nominal load ratios lower than zero, fatigue assessment performed by following the recommendations of the available standard can lead to an excessive level of conservatism. The effect of residual stresses can be mitigated by relieving the material in the

weld regions via appropriate technological processes. However, by so doing, aluminium weldments' fatigue strength is seen to increase, with the role played by non-zero mean stresses becoming more and more important as load ratio R decreases [53].

Both EC9 and the IIW suggest to use specific enhancement factors in order to take into account the effect of the load ratio characterising the load history being assessed. Enhancement factor  $f(R)$  is defined as the ratio between the actual value of the endurance limit at  $2 \cdot 10^6$  cycles to failure and the corresponding design endurance limit recommended as being used for the specific welded geometry being designed. In other words, from a fatigue assessment point of view, under  $R < 0.5$  the fatigue strength of the specific welded detail being designed can be increased by multiplying the corresponding fatigue class by  $f(R)$ .

Both EC9 [46] and the IIW [6] considers the following three scenarios:

- **Case I.** *Un-welded base material and wrought products with negligible residual stresses; stress relieved welded components, in which the effects of constraints or secondary stresses have been considered in analysis; no constraints in assembly:*

$$\begin{aligned}
 f(R) &= 1.6 && \text{for } R < -1 \\
 f(R) &= -0.4 \cdot R + 1.2 && \text{for } -1 \leq R \leq 0.5 \\
 f(R) &= 1 && \text{for } R > 0.5
 \end{aligned} \tag{7}$$

- **Case II.** *Small scale thin-walled simple structural elements containing short welds; parts or components containing thermally cut edges; no constraints in assembly:*

$$\begin{aligned}
 f(R) &= 1.3 && \text{for } R < -1 \\
 f(R) &= -0.4 \cdot R + 0.9 && \text{for } -1 \leq R \leq -0.25 \\
 f(R) &= 1 && \text{for } R > -0.25
 \end{aligned} \tag{8}$$

- **Case III.** *Complex two- or three-dimensional welded components; components with global residual stresses; thick-walled components; normal case for welded components and structures:*

$$f(R) = 1 \quad (9)$$

In order to check the accuracy and reliability of the enhancement factors reported above for Case I and Case II, all the data considered in the present investigation were post-processed to compare the experimental value of  $f(R)$  to the corresponding value estimated according to rules (7) and (8). In particular, independently of type of welded joint and adopted definition for the design stress, the experimental values for the enhancement factors were calculated as follows:

$$f(R) = \frac{\Delta\sigma_{A,97.7\%}|_{\text{experimental}}}{\Delta\sigma_{A,97.7\%}|_{\text{fatigue class}}} \quad \text{or} \quad f(R) = \frac{\Delta\sigma_{A,95\%}|_{\text{experimental}}}{\Delta\sigma_{A,95\%}|_{\text{fatigue class}}} \quad (10)$$

In a similar way, the enhancement factors for the N-SIF approach were determined as:

$$f(R) = \frac{\Delta K_{I,97.7\%}|_{\text{experimental}}}{\Delta K_{I,97.7\%}|_{\text{master curve}}} \quad (11)$$

The results of this analysis are summarised in the  $f(R)$  vs.  $R$  diagrams of Figures 8a to 8f. These charts make it evident that, independently of the adopted design strategy, the experimentally determined values for enhancement factor  $f(R)$  are highly scattered. However, in spite of such a large level of scattering, the diagrams of Figures 8a to 8f confirm that, on average, the fatigue strength of aluminium welded joints tends to increase as the load ratio decreases.

In order to assess the experimental values obtained for  $f(R)$  from the different data sets being re-analysed, in diagrams 8a to 8f also the straight lines plotted according correction rules (7) and (8) are also reported. These charts make it evident that the strategies being suggested both by EC9 and the IIW to enhance the strength of aluminium welded joints subjected to in-service load ratios lower than zero are highly conservative. This precautionary approach is clearly justified by the fact that the effect of non-zero mean stresses on the overall fatigue strength of aluminium welded joints depends on a large number of variable which include, amongst other: technological aspects characterising the specific welding technique being employed, quality of the joints, environmental conditions, and type of applied loading. Accordingly, given a specific welded connection, the only way to accurately quantify its sensitivity to the presence of superimposed static stresses is by running appropriate experiments, with this clearly increasing the time and costs associated with the design problem. However, it has to be said that real structure are seen to be much less sensitive to the presence of non-zero mean stresses than laboratory specimens are [69]. This explains the reason why in situation of practical interest, aluminium welded joints are usually designed by taking the enhancement factor,  $f(R)$ , invariably equal to unity – i.e., Case III, Eq. (9).

To conclude, the chart of Figure 8g plots the experimental values for the negative inverse slope vs. the applied load ratio, the reported  $k$  values being those calculated by post-processing the data sets considered in the present investigation. The above chart makes it evident that, on average, the negative inverse slope is not affected by the applied value of load ratio  $R$ , with this fully confirming the validity of the assumptions on which the standard corrections recommended as being used to take into account the presence of non-zero mean stresses are based. Finally, Figure 8g confirms that the value of 3 suggested by the IIW is conservative, whilst the values for the negative inverse slope supplied by EC9 are capable of capturing the observed experimental reality more accurately.

## 9. Conclusions

- The use of the design curves recommended both by EC9 and the IIW to perform the fatigue assessment of aluminium welded joints according to the Nominal Stress approach is seen to result in an adequate level of accuracy, with the estimates being, on average, conservative.
- The data sets considered in the present investigation fully confirm the fact that the Hot-Spot approach can be used successfully to design real aluminium welded joints against fatigue.
- The Effective Notch Stress approach is seen to be the most accurate design methodology recommended by the IIW. However, it requires intensive computational effort to model weld toes and roots by introducing the required fillet radii (with this holding true especially in the presence of complex three-dimensional welded geometries).
- The re-analysis discussed in the present paper further confirms the notorious accuracy of the N-SIF approach in estimating fatigue lifetime of aluminium welded joints.
- The TCD applied in the form of the PM is seen to be highly accurate in assessing the strength of aluminium welded joints subjected to fatigue loading.
- The TCD can be used in situations of practical interest to design, in terms of maximum principal stress, aluminium welded joints against fatigue by taking the required critical distance value,  $L_{W-Al}$ , invariably equal to 0.5 mm.
- As far as aluminium welded joints are concerned, the enhancement factors recommended both by EC9 and the IIW are seen to result in conservative estimates. Accordingly, experimental trials should be run in order to assess accurately the sensitivity of the specific welded joints being designed to the presence of non-zero mean stresses.

## Appendix A: Statistical determination of fatigue curves

Fatigue curves are schematised as straight lines in a log-log plot (Fig. 1b) and therefore described mathematically via the following well-known Wöhler-type equation:

$$\Delta\sigma^k \cdot N_f = \Delta\sigma_A^k \cdot N_A \quad (\text{A1})$$

where  $\Delta\sigma_A$  is the endurance limit extrapolated at  $N_A$  cycles to failure.

Fatigue curves are usually determined through a least squares linear regression, this optimisation being performed under the hypothesis of a log-normal distribution of the cycles to failure at any stress level (Fig. A1) [70]. Accordingly, for a given number of experimental results, the fatigue curve for a probability of survival,  $P_s$ , equal to 50% is determined by calibrating constants  $c_0$  and  $c_1$  in the following linear regression function:

$$\log(N_f) = c_0 + c_1 \cdot \log(\Delta\sigma) \quad (\text{A2})$$

where  $\Delta\sigma$  is the independent variable and  $N_f$  is the dependent variable.

Assume now that the number of experimental results to be used to calibrate Eq. (A2) is equal to  $n$ . Given the population of data, the  $i$ -th specimen (for  $i=1, 2, \dots, n$ ) is assumed to be tested at a stress level equal to  $\Delta\sigma_i$ , the corresponding experimental number of cycles to failure being equal to  $N_{f,i}$ . Via the least squares method, the values for constants  $c_0$  and  $c_1$  in Eq. (A2) can then be calculated as [71]:

$$c_1 = \frac{\sum_{i=1}^n [\log(\Delta\sigma_i) - x_m] \cdot [\log(N_{f,i}) - y_m]}{\sum_{i=1}^n [\log(\Delta\sigma_i) - x_m]^2} \quad (\text{A3})$$

$$c_0 = y_m - c_1 \cdot x_m \quad (\text{A4})$$

where

$$x_m = \frac{\sum_i^n \log(\Delta\sigma_i)}{n} \quad (A5)$$

$$y_m = \frac{\sum_i^n \log(N_{f,i})}{n} \quad (A6)$$

As soon as constants  $c_0$  and  $c_1$  are known, both the negative inverse slope,  $k$ , and the endurance limit,  $\Delta\sigma_{A,50\%}$ , extrapolated for  $P_S=50\%$  at  $N_A$  cycles to failure can directly be determined by simply rewriting Eq. (A1) in the form of Eq. (A2), obtaining:

$$k = -c_1 \quad (A7)$$

$$\Delta\sigma_{A,50\%} = \left( \frac{10^{c_0}}{N_A} \right)^{\frac{1}{k}} \quad (A8)$$

To determine the scatter band characterising the population of experimental data being post-process, initially the associated standard deviation has to be calculated according to the following standard formula:

$$s = \sqrt{\frac{\sum_{i=1}^n \left\{ \log(N_{f,i}) - \log \left[ N_A \left( \frac{\Delta\sigma_{A,50\%}}{\Delta\sigma_i} \right)^k \right] \right\}^2}{n-1}} \quad (A9)$$

Standard deviation  $s$  allows the endurance limit at  $N_A$  cycles to failure to be estimated directly for  $P_s=P\%$  and  $P_s=(1-P)\%$ , respectively (Fig. A1), i.e.:

$$\Delta\sigma_{A,P\%} = \Delta\sigma_{A,50\%} \left[ \frac{N_A}{10^{\log(N_A)+q \cdot s}} \right]^{1/k} \quad (\text{A10})$$

$$\Delta\sigma_{A,(1-P)\%} = \Delta\sigma_{A,50\%} \left[ \frac{N_A}{10^{\log(N_A)-q \cdot s}} \right]^{1/k}, \quad (\text{A11})$$

In Eqs (A10) and (A11)  $q$  is a statistical index that depends on the adopted confidence level, the chosen probability of survival, and the number of tested samples [48]. Table A1 lists, for different probabilities of survival, some values of index  $q$  determined, under the hypothesis of a log-normal distribution, by taking the confidence level equal to 95% [72].

To conclude, it is worth highlighting that the curves determined for  $P_s$  equal to  $P\%$  and to  $(1-P)\%$  have both negative inverse slope,  $k$ , equal to that of the Wöhler curve determined for  $P_s=50\%$  - Eq. (A8).

## References

- [1] Fricke W. Review Fatigue analysis of welded joints: state of development. *Mar Struc* 2003;16(3):185-200.
- [2] Borrego LP, Costa JD, Jesus JS, Loureiro AR, Ferreira, JM. Fatigue life improvement by friction stir processing of 5083 aluminium alloy MIG butt welds. *Theor Appl Fract Mec* 2014;70:68-74.
- [3] Haryadi GD, Kim SJ. Influences of post weld heat treatment on fatigue crack growth behavior of TIG welding of 6013 T4 aluminium alloy joint (part 1. Fatigue crack growth across the weld metal). *J Mech Sci Technol* 2011;25(9):2161-2170.
- [4] Susmel L. *Multiaxial notch fatigue: from nominal to local stress/strain quantities*. Woodhead Publishing Limited, Cambridge, UK 2009.
- [5] Susmel L. The Modified Wöhler Curve Method calibrated by using standard fatigue curves and applied in conjunction with the Theory of Critical Distances to estimate fatigue lifetime of aluminium weldments. *Int J Fatigue* 2009;31:197-212.

- [6] Hobbacher A. Recommendations For Fatigue Design of Welded Joints and Components IIW document XIII-2151-07/XV-1254-07, 2007.
- [7] Susmel L. Four Stress analysis strategies to use the Modified Wöhler Curve Method to perform the fatigue assessment of weldments subjected to constant and variable amplitude multiaxial fatigue loading. *Int J Fatigue* 2014;67:38-54.
- [8] Aygul M. Fatigue Analysis of Welded Structures Using the Finite Element Method. Ph.D thesis, Chalmers University of Technology, Gothenburg, Sweden, 2012 (available at: <http://publications.lib.chalmers.se/records/fulltext/155710.pdf>)
- [9] Hobbacher AF. New developments at the recent update of the IIW recommendations for fatigue of welded joints and components. *Steel Construction* 2010;3(4):231-242.
- [10] Niemi E, Fricke W, Maddox SJ. Fatigue Analysis of Welded Components: Designer's Guide to the Structural hot spot stress approach (IIW-1430-00). Woodhead Publishing Limited, Cambridge, UK, 2006.
- [11] Niemi E. Structural stress approach to fatigue analysis of welded components. IIW-document XIII-1819-00/XV-1090-01, 2000.
- [12] Morgenstern C, Sonsino CM, Hobbacher A, Sorbo F. Fatigue design of aluminium welded joints by the local stress concept with the fictitious notch radius of  $r_f=1\text{mm}$ . *Int J Fatigue* 2006;28:881-890.
- [13] Karakas O, Morgenstern C, Sonsino CM. Fatigue design of welded joints from the wrought magnesium alloy AZ31 by the local stress concept with the fictitious notch radii of  $r_f=1.0$  and  $0.05\text{mm}$ . *Int J Fatigue* 2008;30:2210-2219.
- [14] Williams ML. Stress singularities resulting from various boundary conditions in angular corners of plates in extension. *J Appl Mech* 1952;19:526-8.
- [15] Lazzarin P, Tovo R. A unified approach to the evaluation of linear elastic stress fields in the neighborhood of cracks and notches. *Int J Fracture* 1996;78:3-19.
- [16] Lazzarin P, Tovo R. A notch intensity factor approach to the stress analysis of welds. *Fatigue Fract Engng Mater Struct* 1998;21:1089-1103.
- [17] Lazzarin P, Lassen T, Livieri P. A notch stress intensity approach applied to fatigue life predictions of welded joints with different local toe geometry. *Fatigue Fract Engng Mater Struct*, 2003;26:49-58.
- [18] Atzori B, Lazzarin P, Meneghetti G. Fatigue Strength Assessments of Welded Joints: from the Integration of Paris' Law to Synthesis Based on the Notch Stress Intensity Factors of the Uncracked Geometries. *Eng Fract Mech* 2008;75(3-4):364-378.
- [19] Taylor D, Barrett N, Lucano G. Some new methods for predicting fatigue in welded joints. *Int J Fatigue* 2002;24:509-518.
- [20] Crupi G, Crupi V, Guglielmino E, Taylor D. Fatigue assessment of welded joints using critical distance and other methods. *Eng Fail Anal* 2005;12:129-142.

- [21] Susmel L, Taylor D. A novel formulation of the theory of critical distances to estimate lifetime of notched components in the medium-cycle fatigue regime. *Fatigue Fract Engng Mater Struct* 2007;30:567-581.
- [22] Livieri P, Lazzarin P. Fatigue strength of steel and aluminium welded joints based on generalised stress intensity factors and local strain energy values. *Int J Fracture* 2005;133(3):247-276.
- [23] Lazzarin P, Livieri P. Notch stress intensity factors and fatigue strength of aluminium and steel welded joints. *Int J Fatigue* 2001;23:225-232.
- [24] Neumann A. Theoretische Grundlagen der Austwertung von Dauerfestigkeitsversuchen aus Schweißverbindungen und geschweißten Bauteilen aus Al Mg- Legierungen *Wissenschaftl. Wissenschaftliche Zeitschrift der Technischen Universität Karl-Marx-Stadt, Chemnitz, Germany, 1965.*
- [25] Anon. Minutes of the meeting of the Working Group on fatigue issues in shipbuilding. The Shipbuilding Engineering Society, Blohm & Voss AG, Hamburg, 1973 ([www.blohmvooss.com](http://www.blohmvooss.com)).
- [26] Person NL, Fatigue of aluminium alloy welded joints. *Welding Research Supplement* 1971;3:77s-87s.
- [27] Wood JL. Flexural fatigue strength of butt welds in Np.5/6 type aluminium alloy. *British Welding Journal* 1970;7(5):365-380.
- [28] Atzori B, Bufano R. Raccolta di dati sulla resistenza a fatica dei giunti saldati in Al Mg5. University of Bari, Bari, Italy, Report no. 76/4, November 1976
- [29] Haibach E, Kobler HG. Beurteilung der Schwingfestigkeit von Schweißverbindungen aus AlZnMg<sub>i</sub> auf dem Weg einer örtlichen Dehnungsmessung. *Aluminium* 1971;47:725-730.
- [30] Mindlin H. Fatigue of Aluminium Magnesium Alloys. *Welding Research Supplement* 1963;1:276-281.
- [31] Gunn KW, McLester R. Effect of Mean Stress on Fatigue Properties of Aluminum Butt-Welded Joints. *Welding Research Abroad*, 1960;6(7):53-60.
- [32] Newman RP. Fatigue tests on butt welded joints in Aluminium Alloys HE.30 and NP. 5/6. *British Welding Journal* 1959;6(7):324-332.
- [33] Gunn KW, Lester MC. Fatigue Strength of welded joints in Aluminium Alloys. *British Welding Journal* 1962;9(12):634-649.
- [34] Jacoby G. Über das Verhalten von Schweißverbindungen aus Aluminiumlegierungen bei Schwingbeanspruchung. Dissertation, Technische Hochschule, Hannover, 1961.
- [35] Andrew RC, Waring J. Axial-Tension Fatigue in Aluminium MIG Welding. *Met Const and Brit Weld Journal* 1974;6:8-11.
- [36] De Money FW, Wolfer GC. Fatigue Properties of plate and Butt Weldment of 5083-H 113 at 75 and- 300F. *Advances in Cryogenic Engineering*, Plenum Press, NY, USA, 1961;6:590-603.

- [37] Haibach E, Atzori B. A Statistical Re-analysis of Fatigue Test Results on Welded Joints in AlMg5. Fraunhofer-Gesellschaft, Report No. FB-116, 1974.
- [38] Kiefer TF, Keys RD, Schwartzberg FR. Determination of low-Temperature Fatigue Properties of Structural Metal Alloys. Martin Company Report CR, pp. 65-70, October 1965.
- [39] Atzori B, Indrio, P. Comportamento a fatica dei ciunti saldati in Al Zn Mg1, Al Zn4 Mg1 ED Al Mg Si. University of Bari, Bari, Italy, Report No. 76/5, December 1976.
- [40] Kosteas D. Zur systematische Auwertung von Schwingfestigkeit von Schwingfestigkeitsuntersuchungen bei Aluminiumlegierungen. Dissertation, University of Munich, Germany, 1970.
- [41] Kosteas D. Versuchsergebnisse aus Schwingfestigkeitsuntersuchungen mit Al Zn Mg1 und Al Mg4.5 Mn. VA Berich NR 5889/2, 25 2, 1973.
- [42] Sidhom N, Laamouri A, Fathallah R, Braham C, Lieurade HP. Fatigue strength improvement of 5083 H11 Al-alloy T-welded joints by shot peening: experimental characterization and predictive approach. *Int J Fatigue* 2005;27:729-745.
- [43] Maddox SJ. Scale effect in fatigue of fillet welded aluminium alloys. Proceedings of the Sixth International Conference on Aluminium Weldments, Cleveland, Ohio, pp. 77-93, 1995
- [44] Meneghetti G. Design approaches for fatigue analysis of welded joints. PhD Thesis, Univeristy of Padova, Padova, Italy, 1998.
- [45] Riberio AS, Goncalves JP, Oliveria F, Castro PT, Fernandes AA. A comparative study on the fatigue behaviour of aluminium alloy welded and bonded Joints. Proceeding of the Sixth International Conference on Aluminium Weldments, Cleveland, Ohio, 65-76.
- [46] Anon. Eurocode 9: Design of aluminium structures – Part 2: Structures susceptible to fatigue, prENV 1999.
- [47] Spindel JE, Haibach E. Some considerations in the statistical determination of the shape of S-N cruves. In: *Statistical Analysis of Fatigue Data*, ASTM STP 744 (Edited by R. E. Little and J. C. Ekvall), pp. 89-113, 1981.
- [48] Hertzberg RW. *Deformation and Fracture Mechanics of Engineering Materials*, 4th edn, Chichester, Wiley, New York, USA, 1996.
- [49] Haibach E. *Service fatigue-strength – methods and data for structural analysis*. VDI, Düsseldorf, Germany, 1992.
- [50] Fricke W. IIW guideline for the assessment of weld root fatigue. *Welding in the World*, 2013;57:753-791.
- [51] Djavit DE, Strande E. Fatigue failure analysis of fillet welded joints used in offshore structures. MSc Thesis, Chalmers University of Technology, Goteborg, Sweden, 2013.
- [52] Radaj D, Sonsino CM, Fricke W. Recent developments in local concepts of fatigue assessment of welded joints. *Int J Fatigue* 2009;31:2-11.

- [53] Radaj D, Sonsino, CM, Fricke W. Fatigue assessment of welded joints by local approaches, Cambridge, England: Woodhead Publishing Limited, 2006.
- [54] Dong P. A Structural stress definition and numerical implementation for fatigue analysis of welded joints. *Int J Fatigue* 2001;23:865-876.
- [55] Sonsino CM. A consideration of allowable equivalent stresses for fatigue design of welded joints according to the notch stress concept with the reference radii  $r_{ref} = 1.00$  and  $0.05$  mm. *Welding in the World* 2009;53(3/4):R64-R75.
- [56] Fricke W. Round-Robin Study on stress analysis for the effective notch stress approach. *Welding in World* 2007;51:68-79.
- [57] Radaj D. Design and analysis of fatigue resistant welded structures. Abington publishing, Cambridge, England, 1990.
- [58] Berto F, Lazzarin P, Radaj D. Fictitious notch rounding concept applied to V-notches with root hole subjected to in-plane mixed mode loading. *Eng Fract Mech* 2014;128:171-188.
- [59] Radaj D, Lazzarin P, Berto F. Generalised Neuber concept of fictitious notch rounding. *Int J Fatigue* 2013;51:Pages 105-115.
- [60] Berto F, Lazzarin P, Radaj D. Application of the fictitious notch rounding approach to notches with end-holes under mode 2 loading. *SDHM Structural Durability and Health Monitoring* 2012;8(1):31-44.
- [61] Berto F, Lazzarin P, Radaj D. Fictitious notch rounding concept applied to V-notches with root holes subjected to in-plane shear loading. *Eng Fract Mech* 2012;79:281-294.
- [62] Atzori B, Lazzarin P, Tovo R. Stress field parameters to predict the fatigue strength of notched components. *J Strain Anal Eng Des* 1999;34(6):437-453.
- [63] Verreman Y, Nie B. Early development of fatigue cracking at manual fillet welds. *Fatigue Fract Engng Mater Struct* 1996;19(6):669-681.
- [64] Radaj D. State-of-the-art review on the local strain energy density concept and its relation to the J-integral and peak stress method. *Fatigue Fract Engng Mater Struct* 2015;38(1):2-28.
- [65] Radaj D. State-of-the-art review on extended stress intensity factor concepts. *Fatigue Fract Engng Mater Struct* 2014;37(1):1-28.
- [66] Peterson RE. Notch Sensitivity. In: *Metal Fatigue*, Edited by G. Sines and J. L. Waisman, McGraw Hill, New York, pp. 293-306, 1959.
- [67] Neuber H. *Theory of Notch stresses: Principles for exact calculation of strength with reference to structural form and material*, Springer Verlag, Berlin, Germany, 1958.
- [68] Tanaka K. Engineering formulae for fatigue strength reduction due to crack-like notches. *Int J Fracture* 1983;22:R39-R45.
- [69] Atzori B. Trattamenti termici e resistenza a fatica delle strutture saldate. *Rivista Italiana della Saldatura*, Edited by A.T.A, Genova, Italy, 1983;1:3-16.

[70] Sinclair GM, Dolan TJ. Effect of stress amplitudes on statistical variability in fatigue life of 75S-T6 Aluminium Alloy. Transaction of the ASME 1953;75:867-872.

[71] Lee Y-L, Pan J, Hathaway R, Barkey M. Fatigue testing and analysis. Butterworth-Heinemann, Elsevier, 2005.

[72] Gibbons Natrella M. Experimental Statistics. National Bureau of Standards, Handbook 91, 1963.

## List of Captions

- Table 1.** *Fatigue results generated by testing ground butt welded joints (geometries Aa and Ae in Figure 1a) statistically re-analysed in terms of nominal stresses.*
- Table 2.** *Fatigue results generated by testing butt welded joints (geometry Ab in Figure 1a) statistically re-analysed in terms of nominal stresses.*
- Table 3.** *Fatigue results generated by testing non-load carrying fillet welded joints (geometries Ba, Bd and Be in Figure 1a) statistically re-analysed in terms of nominal stresses.*
- Table 4.** *Fatigue results generated by testing non-load carrying fillet welded T-joints (geometry Bb in Figure 1a) statistically re-analysed in terms of nominal stresses.*
- Table 5.** *Fatigue results generated by testing cruciform full-penetration welded joints (geometry Ca in Figure 1a) statistically re-analysed in terms of nominal stresses.*
- Table 6.** *Fatigue results generated by testing load carrying fillet cruciform welded joints (geometry Cb in Figure 1a) statistically re-analysed in terms of nominal stresses.*
- Table 7.** *Summary of the statistical re-analyses for the different approaches/welded geometries and corresponding recommended curves.*
- Table 8.** *Fatigue results generated by testing non-load carrying fillet cruciform welded joints (geometry Ba in Figure 1a) statistically re-analysed in terms of hot-spot stresses as well as in terms of local stress quantities.*
- Table 9.** *Fatigue results generated by testing non-load carrying fillet welded T-joints (geometry Bb in Figure 1a) statistically re-analysed in terms of hot-spot stresses as well as in terms of local stress quantities.*
- Table 10.** *Fatigue results generated by testing cruciform full-penetration welded joints (geometry Ca in Figure 1a) statistically re-analysed in terms of hot-spot stresses as well as in terms of local stress quantities.*
- Table 11.** *Fatigue results generated by testing load carrying fillet cruciform welded joints (geometry Cb in Figure 1a) statistically re-analysed in terms of hot-spot stresses as well as in terms of local stress quantities.*
- Table A1.** *Index  $q$  for a confidence level equal to 0.95% [67].*
- Figure 1.** *Geometry of the investigated welded details (a); Wöhler diagram (b).*
- Figure 2.** *Accuracy of the Nominal Stress approach in estimating the fatigue strength of the investigated welded joints - see Fig. 1a for the definition of the different welded geometries.*
- Figure 3.** *Definition of hot-spot stress (a); accuracy of the Hot-Spot Stress approach in estimating the fatigue strength of the investigated welded joints (b) - see Fig. 1a for the definition of the different welded geometries.*
- Figure 4.** *Examples of FE models being solved.*
- Figure 5.** *Weld toe and root rounded according to the reference radius concept (a); accuracy of the Effective Notch Stress approach in estimating the fatigue strength of the investigated welded joints (b) - see Fig. 1a for the definition of the different welded geometries.*
- Figure 6.** *Local stress state in the vicinity of the weld toe (a); accuracy of the N-SIF approach in estimating the fatigue strength of the investigated welded joints (b) - see Fig. 1a for the definition of the different welded geometries.*
- Figure 7.** *Local stress-distance curve and critical distance  $L_{W-AI}$  according to the PM (a); accuracy of the PM in estimating the fatigue strength of the investigated welded joints (b) - see Fig. 1a for the definition of the different welded geometries.*
- Figure 8.** *Effect of load ratio  $R$  on the fatigue strength of aluminium welded joints.*

## Tables

Series	Ref.	No of Data	Load Type <sup>(1)</sup>	R	t [mm]	k	T <sub>σ</sub>	Nominal Stress		Parent material	Filler material
								Δσ <sub>A,50%</sub> [MPa]	Δσ <sub>A,97.7%</sub> [MPa]		
Aa-1	[35]	9	Ax	0	4.8	8.5	2.27	117.3	77.9	5083	5356
Aa-2	[35]	9	Ax	0	4.8	6.9	2.13	116.7	80.0	5083	5356
Aa-3	[35]	9	Ax	0	4.8	10.6	2.89	132.4	77.9	5083	5356
Aa-4	[35]	9	Ax	0	4.8	9.5	3.03	132.5	76.1	5083	5356
Aa-5	[35]	9	Ax	0	4.8	5.9	2.37	110.4	71.6	5083	5356
Aa-6	[35]	9	Ax	0	4.8	14.8	2.18	129.8	87.9	5083	5356
Aa-7	[35]	9	Ax	0	4.8	5.1	2.06	100.6	70.1	5083	5356
Aa-8	[35]	9	Ax	0	4.8	10.6	2.02	127.1	89.3	5083	5356
Aa-9	[35]	9	Ax	0	4.8	7.9	2.78	120.1	72.0	5083	5356
Aa-10	[27]	11	Be	-1	6.4	4.9	1.84	163.0	120.0	NP 5/6	NG 6
Aa-11	[27]	18	Be	-1	6.4	7.2	1.76	189.6	143.0	NP 5/6	NG 6
Aa-12	[27]	8	Be	-1	6.4	5.4	1.28	159.2	140.7	NP 5/6	NG 6
Aa-13	[27]	8	Be	-1	6.4	5.0	2.49	164.0	104.0	NP 5/6	NG 6
Aa-14	[27]	5	Be	-1	6.4	8.2	5.36	236.3	102.0	NP 5/6	NG 6
Aa-15	[27]	7	Be	-1	6.4	3.9	2.25	115.1	76.8	NP 5/6	NG 6
Aa-16	[26]	16	Be	-1	9.5	5.6	1.78	188.3	141.1	5083-H113	5183
Aa-17	[26]	12	Be	-1	9.5	6.4	1.72	211.1	161.1	5456-H321	5556
Aa-18	[37]	10	Be	-1	7.6	7.1	1.92	288.8	208.4	5456-H321	n/a
Aa-19	[36]	12	Be	-1	7.6	11.6	1.20	308.6	281.8	5083-H113	5183
Aa-20	[36]	15	Be	-1	7.6	5.3	1.84	185.6	136.8	5083-H113	5183
Aa-21	[34]	20	Ax	0.08	12.0	4.1	1.80	73.4	54.8	Al Zn Mg1	S-Al Mg5
Aa-22	[26]	9	Ax	0	9.5	5.5	1.51	112.4	91.4	5083-H113	5183
Aa-23	[26]	11	Ax	0	9.5	5.9	1.65	114.3	88.9	5083-H113	5356
Aa-24	[26]	12	Ax	0	9.5	4.7	2.02	99.2	69.9	n/a	n/a
Aa-25	[34]	17	Ax	0	12	4.0	1.63	79.3	62.1	Al Mg5 F28	S-Al Mg5
Aa-26	[30]	8	Ax	0	6.4	8.5	1.12	128.8	121.9	5083-H113	5356
Aa-27	[30]	10	Ax	0	9.5	7.3	1.42	105.0	88.2	5083-H113	5356
Aa-28	[30]	10	Ax	0	9.5	11.1	1.53	128.0	103.4	5083-H113	5356
Ae-1	[37]	9	Ax	0	7.6	10.2	3.08	139.7	79.6	5086-H32	5356
Ae-2	[37]	9	Ax	0	7.6	12.9	1.45	199.6	165.8	5456-H321	5556
Ae-3	[37]	10	Ax	0	7.6	12.3	1.91	162.9	117.8	5456-H321	5556
Ae-4	[37]	8	Ax	0	7.6	9.8	1.89	171.1	124.6	5083-H113	5556
Ae-5	[37]	6	Ax	0	7.6	12.7	3.25	181.3	100.6	5086-H32	5356
Ae-6	[37]	29	Be	-1	7.6	6.7	2.62	229.9	142.0	5083-H112	5556
Ae-7	[37]	28	Be	-1	7.6	8.4	1.74	242.7	184.1	5083-0	5183
Ae-8	[37]	24	Be	-1	7.6	6.9	1.66	221.5	171.8	5083-H112	5183

<sup>(1)</sup>Ax= axial cyclic loading; Be=cyclic bending.

**Table 1.** Fatigue results generated by testing ground butt welded joints (geometries Aa and Ae in Figure 1a) statistically re-analysed in terms of nominal stresses.

Series	Ref.	No of Data	Load Type <sup>(1)</sup>	R	t [mm]	k	T <sub>σ</sub>	Nominal Stress		Parent material	Filler material
								Δσ <sub>A,50%</sub> [MPa]	Δσ <sub>A,97.7%</sub> [MPa]		
Ab-1	[28]	15	Ax	0	9.5	4.4	2.90	56.8	33.4	5083 a 6061	5356
Ab-2	[28]	15	Ax	0	9.5	4.3	2.32	57.9	38.0	5083-H113	5356
Ab-3	[28, 37]	30	Be	-1	4.0	7.1	1.69	191.2	146.9	Al Mg5	Al Mg5
Ab-4	[27]	32	Be	-1	6.4	5.5	1.92	124.6	89.9	NP 5/6	NG 6
Ab-5	[27]	16	Be	-1	6.4	8.8	1.46	182.3	150.9	NP 5/6	NG 6
Ab-6	[27]	13	Be	-1	6.4	5.5	2.06	128.3	89.3	NP 5/6	NG 6
Ab-7	[27]	8	Be	-1	6.4	3.6	1.85	108.7	79.8	NP 5/6	NG 6
Ab-8	[27]	11	Be	-1	6.4	4.6	2.14	147.8	101.0	NP 5/6	NG 6
Ab-9	[27]	11	Be	-1	6.4	4.9	2.68	122.1	74.6	NP 5/6	NG 6
Ab-10	[26]	14	Be	-1	9.5	5.4	1.72	136.8	104.3	5083-H113	5183
Ab-11	[26]	14	Be	-1	6.4	4.7	1.82	121.6	90.2	5456-H321	5556
Ab-12	[38]	12	Ax	-1	2.5	7.5	2.44	251.5	161.1	5456-H321	5556
Ab-13	[38]	12	Ax	-1	2.5	6.0	1.69	164.8	126.8	5456-H343	5556
Ab-14	[38]	12	Ax	-1	2.5	6.0	1.80	135.3	100.8	5456-H343	5556
Ab-15	[36]	13	Be	-1	9.5	5.5	2.84	189.0	112.1	5083-H113	5183
Ab-16	[36]	13	Be	-1	9.5	5.4	1.80	136.2	101.4	5083-H113	5183
Ab-17	[36]	13	Be	-1	9.5	5.4	2.02	165.4	116.5	n/a	n/a
Ab-18	[28, 37]	30	Ax	-1	4.0	4.0	2.47	64.4	41.0	Al Mg5	Al Mg5
Ab-19	[28, 37]	18	Ax	-1	4.0	4.6	2.53	106.7	67.0	Al Mg5	Al Mg5
Ab-20	[28, 37]	20	Ax	-1	4.0	5.7	1.88	121.8	88.9	Al Mg5	Al Mg5
Ab-21	[28, 37]	12	Ax	-1	4.0	2.0	13.31	41.9	11.5	Al Mg5	Al Mg5
Ab-22	[28, 37]	12	Ax	-1	4.0	4.4	3.21	104.2	58.1	Al Mg5	Al Mg5
Ab-23	[28, 37]	12	Ax	-1	4.0	5.5	1.87	104.1	76.1	Al Mg5	Al Mg5
Ab-24	[28, 37]	12	Ax	-1	4.0	4.5	2.86	95.2	56.3	Al Mg5	Al Mg5
Ab-25	[28, 37]	12	Ax	-1	4.0	4.5	2.08	99.8	69.3	Al Mg5	Al Mg5
Ab-26	[28, 37]	12	Ax	-1	4.0	6.2	2.19	100.5	68.0	Al Mg5	Al Mg5
Ab-27	[28, 37]	13	Ax	-1	4.0	4.6	3.72	90.8	47.1	Al Mg5	Al Mg5
Ab-28	[28, 37]	14	Ax	-1	4.0	3.1	9.43	60.4	19.7	Al Mg5	Al Mg5
Ab-29	[28, 37]	15	Ax	-1	6.4	10.1	2.18	126.3	85.5	D54 S M	A 56 S
Ab-30	[28, 37]	18	Ax	-1	5.0	5.1	1.85	86.5	63.6	S-AlMg4.5MnF30	S-Al Mg5
Ab-31	[28, 37]	30	Ax	0	4.0	3.9	2.51	46.0	29.0	Al Mg5	Al Mg5
Ab-32	[26]	9	Ax	0	9.5	6.3	2.65	83.4	51.2	5083-H113	5183
Ab-33	[26]	17	Ax	0	9.5	5.1	1.83	65.6	48.5	5083-H113	5356
Ab-34	[26]	10	Ax	0	9.5	4.7	1.58	74.3	59.2	5086-H32	5356
Ab-35	[34]	30	Ax	0	12.0	4.4	2.06	52.0	36.2	Al Mg5 F28	S-Al Mg5
Ab-36	[31]	15	Ax	0	6.4	4.8	2.88	73.1	43.1	D54 S M	A 56 S
Ab-37	[31]	50	Ax	0	10.0	5.8	1.47	86.4	71.4	S-AlMg4.5MnF28	S-AlMg4.5Mn
Ab-38	[32]	17	Ax	0	6.4	6.3	2.42	100.3	64.6	NP 5/6 M	NG 6
Ab-39	[32]	10	Ax	0	6.4	4.6	2.03	71.1	49.8	NP 5/6 M	NG 6
Ab-40	[30]	15	Ax	0	4.8	5.4	1.95	84.1	60.2	5083-H113	5356
Ab-41	[30]	12	Ax	0	6.4	10.6	1.59	112.1	88.9	5083-H113	5356
Ab-42	[30]	21	Ax	0	9.5	8.4	1.83	102.9	75.9	5083-H113	5356
Ab-43	[30]	18	Ax	0	9.5	4.1	1.39	60.8	51.6	5083-H113	5356
Ab-44	[30]	14	Ax	0	6.4	3.1	5.58	58.3	24.7	5083-H113	5356
Ab-45	[30]	15	Ax	0	6.4	3.2	2.53	51.9	32.6	5083-H113	5356
Ab-46	[31]	9	Ax	-0.4	6.4	5.4	4.10	105.3	52.0	D54 S M	A 56 S
Ab-47	[31]	16	Ax	-0.2	6.4	6.6	3.16	96.6	54.3	D54 S M	A 56 S
Ab-48	[31]	11	Ax	0.2	6.4	6.0	1.59	72.3	57.4	D54 S M	A 56 S
Ab-49	[30]	14	Ax	0.25	4.8	7.0	1.36	75.9	65.0	5083-H113	5356
Ab-50	[30]	12	Ax	0.25	6.4	8.2	1.40	89.1	75.2	5083-H113	5356
Ab-51	[30]	18	Ax	0.25	9.5	9.0	1.47	87.1	71.9	5083-H113	5356
Ab-52	[30]	21	Ax	0.25	9.5	5.0	1.53	60.3	48.8	5083-H113	5356
Ab-53	[31]	16	Ax	0.4	6.4	4.3	1.84	61.1	45.1	D54 S M	A 56 S
Ab-54	[34]	7	Ax	0.5	4.8	5.8	1.38	63.6	54.1	5083-H113	5356
Ab-55	[30]	14	Ax	0.5	6.4	10.9	1.42	75.9	63.7	5083-H113	5356
Ab-56	[30]	12	Ax	0.5	9.4	6.4	1.67	66.8	51.6	5083-H113	5356
Ab-57	[30]	21	Ax	0.5	9.5	5.2	1.93	56.3	40.5	5083-H113	5356
Ab-58	[30]	17	Ax	0.6	6.4	6.6	2.11	65.4	45.0	D54 S M	A 56 S

Ab-59	[39]	48	Ax	0	4.0	6.6	1.71	97.6	74.7	Al Mg Si	Al Si5
Ab-60	[39]	9	Ax	0	4.0	7.4	2.17	101.6	68.9	Al Mg Si	Al Mg5
Ab-61	[39]	43	Be	0	4.0	4.4	1.72	149.6	114.0	Al Mg Si	Al Si5
Ab-62	[39]	57	Ax	-1	4.0	7.7	1.89	135.7	98.7	Al Mg Si	Al Si5
Ab-63	[39]	12	Ax	-1	4.0	6.6	1.59	125.2	99.4	Al Mg Si	Al Mg5
Ab-64	[39]	18	Ax	-1	4.0	5.0	1.66	111.1	86.2	Al Mg Si	Al Si5
Ab-65	[39]	12	Ax	-1	8.0	4.4	1.45	136.8	113.6	Al Mg Si	Al Si5
Ab-66	[39]	10	Ax	-1	8.0	5.6	2.16	140.3	95.4	Al Mg Si	Al Si5
Ab-67	[39]	55	Be	-1	4.0	5.7	1.56	169.6	135.9	Al Mg Si	Al Si5
Ab-68	[39]	22	Be	-1	4.0	4.4	1.70	159.6	122.5	Al Mg Si	Al Si5
Ab-69	[39]	27	Be	-1	8.0	5.1	1.48	167.3	137.4	Al Mg Si	Al Si5
Ab-70	[39]	22	Be	-1	4.0	4.4	1.47	166.1	137.2	Al Mg Si	Al Si5
Ab-71	[39]	30	Be	-1	4.0	3.2	1.86	152.5	111.9	Al Mg Si	Al Si5
Ab-72	[34]	21	Ax	0.08	12.0	5.2	1.55	74.2	59.5	Al Zn Mg1	Al Mg7
Ab-73	[34]	23	Ax	0.08	12.0	6.1	1.74	89.1	67.5	Al Zn Mg1	S-Al Mg5
Ab-74	[41]	82	Ax	0.1	6.0	3.9	2.43	57.1	36.7	Al Zn Mg1	Al Mg5
Ab-75	[41]	33	Ax	0.1	6.0	2.9	3.07	52.0	29.7	Al Zn Mg1	Al Mg5
Ab-76	[40]	26	Ax	0.1	10.0	3.8	2.02	61.0	43.0	Al Zn Mg1	Al Mg5
Ab-77	[39]	50	Ax	-1	4.0	4.6	3.42	137.5	74.4	Al Zn4 Mg1	Al Mg5
Ab-78	[39]	18	Ax	-1	4.0	3.8	2.05	125.8	87.8	Al Zn4 Mg1	Al Mg5
Ab-79	[39]	18	Ax	-1	8.0	2.8	2.72	105.9	64.2	Al Zn4 Mg1	Al Mg5

<sup>(1)</sup>Ax= axial cyclic loading; Be=cyclic bending.

**Table 2.** *Fatigue results generated by testing butt welded joints (geometry Ab in Figure 1a) statistically re-analysed in terms of nominal stresses.*

Series	Ref.	No of Data	Load Type <sup>(1)</sup>	R	t [mm]	L [mm]	Z [mm]	k	T <sub>σ</sub>	Nominal Stress		Parent material	Filler material
										Δσ <sub>A,50%</sub> [MPa]	Δσ <sub>A,97.7%</sub> [MPa]		
Ba-1	[28]	10	Be	-1	8.0	8.0	7.7	4.7	1.48	104.4	85.9	Al Mg5	Al Mg5
Ba-2	[28]	10	Ax	-1	8.0	8.0	-	3.5	3.44	88.9	47.9	Al Mg5	Al Mg5
Ba-3	[33]	16	Ax	-1	6.4	12.7	-	3.1	3.74	75.6	39.1	D54 S M	A 56 S
Ba-4	[28]	10	Ax	0	8.0	8.0	-	5.5	2.23	82.5	55.3	Al Mg5	Al Mg5
Ba-5	[33]	17	Ax	0	6.4	12.7	-	3.4	6.37	57.8	22.9	D54 S M	A 56 S
Ba-6	[33]	10	Ax	0.7	6.4	12.7	-	2.9	6.39	32.9	13.0	D54 S M	A 56 S
Ba-7	[39]	11	Ax	0	8.0	8.0	7.7	2.9	7.01	66.4	25.1	Al Mg Si	Al Si5
Ba-8	[39]	10	Be	0	8.0	8.0	7.7	5.8	1.45	124.0	102.8	Al Mg Si	Al Si5
Ba-9	[39]	15	Ax	-1	8.0	8.0	7.7	3.7	1.84	70.2	51.8	Al Mg Si	Al Si5
Ba-10	[30]	10	Be	-1	8.0	8.0	7.7	5.2	1.36	160.7	137.6	Al Mg Si	Al Si5
Ba-11	[40]	29	Ax	0.1	6.0	6.0	-	3.5	2.05	65.3	45.6	Al Zn Mg1	Al Mg5
Ba-12	[40]	27	Ax	0.1	10.0	10.0	-	3.5	2.12	53.5	36.7	Al Zn Mg1	Al Mg5
Ba-13	[39]	18	Ax	0	8.0	8.0	7.7	5.3	1.37	101.8	87.0	Al Zn4 Mg1	Al Mg5
Ba-14	[39]	18	Ax	-1	8.0	8.0	7.7	5.0	1.36	145.1	124.6	Al Zn4 Mg1	Al Mg5
Ba-15	[43]	6	Ax	0.1	3.0	3.0	4.5	4.3	2.19	58.2	39.3	6061-T6	6061-T6
Ba-16	[43]	6	Ax	0.1	6.0	6.0	7.0	4.2	2.18	41.0	27.8	6061-T6	6061-T6
Ba-17	[43]	4	Ax	0.1	12.0	12.0	10.0	3.8	2.27	37.5	24.9	6061-T6	6061-T6
Ba-18	[43]	8	Ax	0.1	24.0	24.0	20.5	3.7	1.54	29.6	23.8	6061-T6	6061-T6
Ba-19	[43]	7	Ax	0.1	24.0	6.0	7.0	3.8	1.48	39.0	32.1	6061-T6	6061-T6
Ba-20	[43]	9	Ax	0.1	12.0	6.0	7.0	3.7	1.56	30.4	24.3	6061-T6	6061-T6
Bd-1	[35]	8	Ax	0	9.5	9.5	-	3.4	3.69	28.1	14.7	NP 5/6 M	NG 6
Bd-2	[35]	6	Ax	0	9.5	9.5	-	3.3	2.47	32.5	20.7	NP 5/6 M	NG 6
Bd-3	[35]	8	Ax	0	9.5	9.5	-	3.8	3.55	64.6	53.6	NP 5/6 M	NG 6
Be-1	[29]	6	Be	0	10.0	-	-	-	-	-	-	Al Zn Mg1	S-ALMg4.5 Mn
Be-2	[20]	25	Be	-1	10.0	-	-	4.5	1.28	156.2	133.6	Al Zn Mg1	S-ALMg4.5 Mn

<sup>(1)</sup>Ax= axial cyclic loading; Be=cyclic bending.

**Table 3.** Fatigue results generated by testing non-load carrying fillet welded joints (geometries Ba, Bd and Be in Figure 1a) statistically re-analysed in terms of nominal stresses.

Series	Ref.	No of Data	Load Type <sup>(1)</sup>	R	Nominal Stress							Parent material	Filler material
					t [mm]	L [mm]	Z [mm]	k	T <sub>σ</sub>	Δσ <sub>A,50%</sub> [MPa]	Δσ <sub>A,97.7%</sub> [MPa]		
Bb-1	[28]	30	Be	0	4.0	4.0	4.2	4.6	1.70	79.1	60.7	Al Mg5	Al Mg5
Bb-2	[28]	30	Be	0	8.0	8.0	7.7	4.1	1.98	73.5	52.2	Al Mg5	Al Mg5
Bb-3	[28]	30	Be	-1	4.0	4.0	4.2	4.5	2.06	94.8	66.1	Al Mg5	Al Mg5
Bb-4	[28]	30	Be	-1	8.0	8.0	7.7	5.1	1.22	103.3	93.7	Al Mg5	Al Mg5
Bb-5	[28]	10	Ax	-1	4.0	4.0	-	6.5	1.83	141.3	104.4	Al Mg5	Al Mg5
Bb-6	[28]	29	Ax	-1	8.0	8.0	-	6.6	1.66	125.7	97.5	Al Mg5	Al Mg5
Bb-7	[28]	10	Ax	-1	8.0	4.0	-	7.1	1.68	132.7	102.5	Al Mg5	Al Mg5
Bb-8	[28]	28	Ax	0	4.0	4.0	-	8.8	1.51	102.5	83.5	Al Mg5	Al Mg5
Bb-9	[28]	27	Ax	0	8.0	8.0	-	7.5	1.46	91.2	75.4	Al Mg5	Al Mg5
Bb-10	[28]	10	Ax	0	8.0	4.0	-	7.8	1.88	111.7	81.6	Al Mg5	Al Mg5
Bb-11	[39]	27	Ax	0	4.0	4.0	4.2	7.3	1.36	105.2	90.4	Al Mg Si	Al Si5
Bb-12	[39]	29	Ax	0	8.0	8.0	7.7	7.0	1.62	79.3	62.2	Al Mg Si	Al Si5
Bb-13	[39]	15	Ax	0	8.0	4.0	7.7	6.7	1.91	85.2	61.6	Al Mg Si	Al Si5
Bb-14	[39]	28	Be	0	4.0	4.0	4.2	6.0	1.36	143.4	122.8	Al Mg Si	Al Si5
Bb-15	[39]	36	Be	0	8.0	8.0	7.7	4.6	1.72	94.7	72.2	Al Mg Si	Al Si5
Bb-16	[39]	27	Ax	-1	4.0	4.0	4.2	7.1	1.48	146.0	120.1	Al Mg Si	Al Si5
Bb-17	[39]	9	Ax	-1	4.0	4.0	4.2	8.9	1.23	147.0	132.4	Al Mg Si	Al Si5
Bb-18	[39]	34	Ax	-1	8.0	8.0	7.7	6.0	1.79	115.3	86.2	Al Mg Si	Al Si5
Bb-19	[39]	21	Ax	-1	8.0	4.0	7.7	5.1	2.56	111.7	69.9	Al Mg Si	Al Si5
Bb-20	[39]	30	Be	-1	4.0	4.0	4.2	5.8	1.56	176.0	140.8	Al Mg Si	Al Si5
Bb-21	[39]	9	Be	-1	4.0	4.0	4.2	6.8	1.28	153.7	135.6	Al Mg Si	Al Si5
Bb-22	[39]	30	Be	-1	8.0	8.0	7.7	5.3	1.51	143.3	116.8	Al Mg Si	Al Si5
Bb-23	[29]	7	Be	0	10.0	10.0	-	8.0	2.13	152.6	104.5	Al Zn Mg1	S-AlMg4.5Mn
Bb-24	[29]	9	Ax	0	10.0	-	-	4.8	1.27	85.3	75.6	Al Zn Mg1	S-AlMg4.5Mn
Bb-25	[29]	33	Be	-1	10.0	10.0	-	5.5	1.29	142.1	125.2	Al Zn Mg1	S-AlMg4.5Mn
Bb-26	[29]	9	Ax	-1	10.0	10.0	-	5.0	1.83	114.6	84.8	Al Zn Mg1	S-AlMg4.5Mn
Bb-27	[39]	27	Ax	0	8.0	8.0	7.7	7.6	1.39	134.0	113.6	Al Zn4 Mg1	Al Mg5
Bb-28	[39]	18	Ax	0	8.0	4.0	7.7	7.6	1.26	139.2	123.9	Al Zn4 Mg1	Al Mg5
Bb-29	[39]	26	Ax	-1	8.0	8.0	7.7	5.5	4.43	170.8	81.2	Al Zn4 Mg1	Al Mg5
Bb-30	[39]	18	Ax	-1	8.0	4.0	7.7	6.6	1.35	195.9	168.5	Al Zn4 Mg1	Al Mg5
Bb-31	[44]	11	Be	0.1	10.0	10.0	7.0	3.9	1.64	41.3	32.3	5083-H11	5183
Bb-32	[44]	15	Be	0.5	10.0	10.0	7.0	3.3	1.64	36.6	28.6	5083-H11	5183
Bb-33	[45]	11	Ax	0.1	12.0	10.0	8.0	4.2	1.46	45.7	37.8	5083-H3	5083-H3
Bb-34	[45]	13	Ax	0.1	12.0	10.0	8.0	4.0	1.38	42.0	35.8	5083-H3	5083-H3
Bb-35	[34]	7	Ax	0.1	12.0	12.0	8.0	4.6	3.78	53.0	27.3	6061-T651	6061-T652

<sup>(1)</sup>Ax= axial cyclic loading; Be=cyclic bending.

**Table 4.** Fatigue results generated by testing non-load carrying fillet welded T-joints (geometry Bb in Figure 1a) statistically re-analysed in terms of nominal stresses.

Series	Ref.	No of Data	Load Type <sup>(1)</sup>	R	t [mm]	L [mm]	Z [mm]	k	T <sub>σ</sub>	Nominal Stress		Parent material	Filler material
										Δσ <sub>A,50%</sub> [MPa]	Δσ <sub>A,97.7%</sub> [MPa]		
Ca-1	[28]	30	Be	0	8.0	4.0	7.7	4.0	1.67	75.5	58.5	Al Mg5	Al Mg5
Ca-2	[28]	30	Be	-1	8.0	4.0	7.7	3.7	1.52	87.5	71.0	Al Mg5	Al Mg5
Ca-3	[28]	9	Be	-1	8.0	8.0	7.7	4.0	1.59	95.9	76.0	Al Mg5	Al Mg5
Ca-4	[28]	10	Be	-1	8.0	4.0	7.7	2.7	2.28	93.6	62.0	Al Mg5	Al Mg5
Ca-5	[28]	29	Ax	-1	8.0	4.0	-	4.0	1.94	57.6	41.4	Al Mg5	Al Mg5
Ca-6	[28]	10	Ax	-1	8.0	4.0	-	2.6	3.09	67.9	38.6	Al Mg5	Al Mg5
Ca-7	[28]	10	Ax	-1	8.0	4.0	-	3.9	1.66	52.7	40.8	Al Mg5	Al Mg5
Ca-8	[28]	29	Ax	0	8.0	4.0	-	4.3	2.81	30.3	18.1	Al Mg5	Al Mg5
Ca-9	[39]	30	Ax	0	8.0	4.0	7.7	4.9	1.74	50.7	38.5	Al Mg Si	Al Si5
Ca-10	[39]	32	Be	0	8.0	4.0	7.7	5.3	2.01	123.5	87.1	Al Mg Si	Al Si5
Ca-11	[39]	31	Ax	-1	8.0	4.0	7.7	4.6	2.07	76.4	53.1	Al Mg Si	Al Si5
Ca-12	[39]	13	Ax	-1	8.0	4.0	7.7	4.6	7.61	61.8	22.4	Al Mg Si	Al Mg5
Ca-13	[39]	12	Ax	-1	8.0	4.0	7.7	3.5	4.03	95.0	47.4	Al Mg Si	Al Si5
Ca-14	[39]	12	Ax	-1	8.0	4.0	7.7	3.9	4.57	48.3	22.6	Al Mg Si	Al Si5
Ca-15	[39]	27	Be	-1	8.0	4.0	7.7	5.1	1.39	148.6	126.0	Al Mg Si	Al Si5
Ca-16	[39]	9	Be	-1	8.0	4.0	7.7	6.3	1.75	151.5	114.4	Al Mg Si	Al Si5
Ca-17	[39]	9	Be	-1	8.0	4.0	7.7	7.2	1.55	152.7	122.7	Al Mg Si	Al Si5
Ca-18	[39]	9	Be	-1	8.0	4.0	7.7	6.6	1.49	163.0	133.8	Al Mg Si	Al Mg5
Ca-19	[34]	16	Ax	0.08	12.0	12.0	-	4.8	1.36	61.9	53.0	Al Zn Mg1	Al Si5
Ca-20	[34]	8	Ax	0.08	12.0	12.0	-	4.6	2.47	53.5	34.0	Al Zn Mg1	Al Si5
Ca-21	[39]	27	Ax	-1	8.0	4.0	-	4.9	1.80	112.0	83.5	Al Zn4 Mg1	Al Mg5
Ca-22	[39]	18	Ax	-1	8.0	8.0	-	5.4	1.45	153.0	126.9	Al Zn4 Mg1	Al Mg5
Ca-23	[39]	18	Ax	-1	8.0	4.0	-	2.9	3.78	93.1	47.9	Al Zn4 Mg1	Al Mg5
Ca-24	[39]	18	Ax	-1	8.0	4.0	-	4.9	1.40	119.1	100.6	Al Zn4 Mg1	Al Si5

<sup>(1)</sup>Ax=axial cyclic loading; Be=cyclic bending.

**Table 5.** Fatigue results generated by testing cruciform full-penetration welded joints (geometry Ca in Figure 1a) statistically re-analysed in terms of nominal stresses.

Series	Ref.	No of Data	Load Type <sup>(1)</sup>	R	t [mm]	L [mm]	Z [mm]	k	T <sub>σ</sub>	Nominal Stress		Parent material	Filler material
										Δσ <sub>A,50%</sub> [MPa]	Δσ <sub>A,97.7%</sub> [MPa]		
Cb-1	[28]	27	Ax	-1	4.0	4.0	-	4.8	1.86	84.8	62.2	Al Mg5	Al Mg5
Cb-2	[28]	29	Ax	-1	8.0	8.0	-	3.8	1.77	69.3	52.1	Al Mg5	Al Mg5
Cb-3	[33]	9	Ax	-1	6.4	12.7	-	4.5	2.41	75.9	48.9	D54 S M	A 56 S
Cb-4	[28]	27	Ax	0	4.0	4.0	-	4.8	2.16	54.3	37.0	Al Mg5	Al Mg5
Cb-5	[28]	30	Ax	0	8.0	8.0	-	4.3	1.88	39.5	28.8	Al Mg5	Al Mg5
Cb-6	[33]	20	Ax	0	6.4	12.7	-	5.0	4.61	49.6	23.1	D54 S M	A 56 S
Cb-7	[33]	25	Ax	0	10.0	10.0	-	3.4	1.26	28.6	25.5	Al Mg5 F28	S-ALMg4.5Mn
Cb-8	[33]	10	Ax	0.6	6.4	12.7	-	5.0	1.83	42.5	31.4	D54 S M	A 56 S
Cb-9	[33]	6	Ax	0.75	6.4	12.7	-	2.9	2.38	33.7	21.9	D54 S M	A 56 S
Cb-10	[39]	31	Ax	0	4.0	4.0	4.2	6.0	1.84	72.0	53.1	Al Mg Si	Al Si5
Cb-11	[39]	23	Ax	0	8.0	8.0	7.7	6.0	1.49	50.2	41.1	Al Mg Si	Al Si5
Cb-12	[39]	25	Ax	0	8.0	8.0	7.7	5.9	1.51	42.9	34.9	Al Mg Si	Al Si5
Cb-13	[39]	27	Ax	-1	4.0	4.0	4.2	6.5	1.76	114.2	86.0	Al Mg Si	Al Si5
Cb-14	[39]	11	Ax	-1	4.0	8.0	4.2	5.8	2.47	105.1	66.9	Al Mg Si	Al Si5
Cb-15	[39]	28	Ax	-1	8.0	8.0	7.7	4.4	1.98	66.9	47.5	Al Mg Si	Al Si5
Cb-16	[34]	12	Ax	0.08	12.0	12.0	6.3	5.8	1.40	38.9	32.9	Al Zn Mg1	Al Si5
Cb-17	[34]	14	Ax	0.08	12.0	12.0	6.3	4.6	1.36	36.2	31.0	Al Zn Mg1	Al Si5
Cb-18	[40]	29	Ax	0.1	6.0	6.0	-	5.3	1.77	54.9	41.2	Al Zn Mg1	Al Si5
Cb-19	[39]	27	Ax	0	4.0	4.0	4.2	3.5	1.86	65.9	48.3	Al Zn4 Mg1	Al Mg5
Cb-20	[39]	27	Ax	0	8.0	8.0	7.7	4.2	2.14	50.0	34.2	Al Zn4 Mg1	Al Mg5
Cb-21	[39]	18	Ax	0	8.0	-	-	4.1	2.32	43.5	28.6	Al Zn4 Mg1	Al Mg5
Cb-22	[39]	27	Ax	-1	8.0	8.0	7.7	3.5	3.43	92.3	49.8	Al Zn4 Mg1	Al Mg5
Cb-23	[42]	12	Ax	0.1	12.0	12.0	8.0	5.3	2.17	29.5	20.0	6061-T651	6061-T652
Cb-24	[42]	18	Ax	0.1	12.0	12.0	6.4	4.4	1.47	27.4	22.6	Al Zn Mg1	Al Zn Mg2
Cc-1	[39]	30	Be	0	4.0	8.0	-	4.7	1.83	119.4	88.3	Al Mg Si	Al Si5
Cc-2	[39]	11	Be	0	4.0	8.0	-	5.5	1.78	133.8	100.3	Al Mg Si	Al Si5
Cc-3	[39]	28	Be	0	8.0	8.0	-	3.9	1.66	92.8	72.0	Al Mg Si	Al Si5
Cc-4	[39]	29	Be	-1	4.0	8.0	-	4.1	1.55	144.4	116.1	Al Mg Si	Al Si5
Cc-5	[39]	12	Be	-1	4.0	8.0	-	6.5	1.42	165.1	138.6	Al Mg Si	Al Si5

<sup>(1)</sup>Ax=axial cyclic loading; Be=cyclic bending.

**Table 6.** Fatigue results generated by testing load carrying fillet cruciform welded joints (geometry Cb in Figure 1a) statistically re-analysed in terms of nominal stresses.

Approach	Welded Geometry	Nominal Stress				EC9		IIW	
		$\Delta\sigma_{A,50\%}^{(1)}$	$\Delta\sigma_{A,97.7\%}^{(2)}$	k	$T_{\sigma}^{(3)}$	$\Delta\sigma_{A,97.7\%}$	k	$\Delta\sigma_{A,95\%}$	k
		[MPa]	[MPa]			[MPa]		[MPa]	
Nominal Stress	Aa	72.1	13.0	1.8	30.88	55	4.5	45	3
	Ab	65.0	17.3	2.4	14.21	36	4.3	36	3
	Ae	185.3	89.2	7.0	4.32	55	4.5	45	3
	Ba	45.7	15.5	2.1	8.69	23	3.4	36	3
	Bb	73.3	22.6	2.5	10.53	23	3.4	36	3
	Bd	30.8	6.5	2.0	22.31	23	3.4	36	3
	Be	54.5	7.6	1.9	51.79	23	3.4	36	3
	Ca	40.1	6.6	1.8	36.60	36	3.4	32	3
	Cb	36.3	11.6	2.7	9.81	25	3.4	36	3
	Cc	109.8	67.2	3.8	2.67	25	3.4	36	3
Hot-Spot Stress	Ba	51.2	13.3	1.9	14.87	-	-	40	3
	Bb	75.8	20.1	2.2	14.30	-	-	40	3
	Ca	65.4	17.3	2.2	14.36	-	-	40	3
	Cb	40.7	11.4	2.4	12.67	-	-	36	3
Effective Notch Stress	Ba $\geq$ 5	113.2	35.1	2.0	10.40	-	-	71	3
	Ba $<$ 5	314.6	85.1	4.3	2.13	-	-	180	3
	Bb $\geq$ 5	145.7	33.3	2.0	19.17	-	-	71	3
	Bb $<$ 5	218.9	85.9	3.1	6.50	-	-	180	3
	Ca $\geq$ 5	129.8	34.0	2.2	14.55	-	-	71	3
	Cb $\geq$ 5	121.3	40.8	2.7	8.83	-	-	71	3
	Cb $<$ 5	297.9	26.2	2.5	20.05	-	-	180	3
N-SIF	Ba	119.5	43.7	2.3	7.46	-	-	-	-
	Bb	150.4	34.9	2.1	18.57	-	-	-	-
	Ca	112.0	21.6	1.9	26.91	-	-	-	-
	Cb	120.7	48.9	3.0	6.09	-	-	-	-
TCD	Ba	80.0	29.0	2.3	7.62	-	-	-	-
	Bb	88.5	16.8	1.8	27.74	-	-	-	-
	Ca	89.2	23.4	2.2	14.60	-	-	-	-
	Cb	81.4	33.0	3.0	6.09	-	-	-	-

<sup>(1)</sup> $\Delta K_{I,50\%}$  at  $2 \cdot 10^6$  cycles to failure for the N-SIF approach measured in units of  $\text{MPa} \cdot \text{mm}^{0.326}$ .

<sup>(2)</sup> $\Delta K_{I,97.7\%}$  at  $2 \cdot 10^6$  cycles to failure for the N-SIF approach measured in units of  $\text{MPa} \cdot \text{mm}^{0.326}$ .

<sup>(3)</sup> $T_{\sigma} = \Delta K_{I,90\%} / \Delta K_{I,10\%}$  for the N-SIF approach.

**Table 7.** Summary of the statistical re-analyses for the different approaches/welded geometries and corresponding recommended curves.

Series	Ref.	No of Data	Load Type <sup>(1)</sup>	R	t	L	Z	k	$T_{\sigma}^{(2)}$	Hot-Spot Stress		Effective Notch Stress		N-SIF		TCD	
					[mm]	[mm]	[mm]			$\Delta\sigma_{A,50\%}$	$\Delta\sigma_{A,97.7\%}$	$\Delta\sigma_{A,50\%}$	$\Delta\sigma_{A,97.7\%}$	$\Delta K_{I,50\%}$	$\Delta K_{I,97.7\%}$	$\Delta\sigma_{A,50\%}$	$\Delta\sigma_{A,97.7\%}$
Ba-1	[28]	10	Be	-1	8.0	8.0	7.7	4.7	1.48	129.8	106.8	244.3	200.9	184.8	152.0	124.6	102.5
Ba-7	[39]	11	Ax	0	8.0	8.0	7.7	2.9	7.01	76.4	28.9	155.3	58.6	156.4	59.1	105.5	39.8
Ba-8	[39]	10	Be	0	8.0	8.0	7.7	5.8	1.45	142.6	118.3	290.0	240.5	219.7	182.2	148.1	122.9
Ba-9	[39]	15	Ax	-1	8.0	8.0	7.7	3.7	1.84	80.8	59.6	164.3	121.1	165.5	122.0	111.6	82.3
Ba-10	[39]	10	Be	-1	8.0	8.0	7.7	5.2	1.36	184.9	158.3	375.9	321.9	284.8	243.9	192.0	164.4
Ba-13	[39]	18	Ax	0	8.0	8.0	7.7	5.3	1.37	126.6	108.2	238.2	203.6	240.0	205.1	161.8	138.3
Ba-14	[39]	18	Ax	-1	8.0	8.0	7.7	5.0	1.36	180.4	154.9	339.4	291.4	342.0	293.6	230.6	197.9
Ba-15	[43]	6	Ax	0.1	3.0	3.0	4.5	4.3	2.19	81.9	55.3	124.1	83.8	124.7	84.2	84.4	57.0
Ba-16	[43]	6	Ax	0.1	6.0	6.0	7.0	4.2	2.18	58.4	39.6	110.6	75.0	110.2	74.7	75.1	49.1
Ba-17	[43]	4	Ax	0.1	12.0	12.0	10.0	3.8	2.27	55.1	36.6	125.9	83.6	127.5	84.7	86.0	57.1
Ba-18	[43]	8	Ax	0.1	24.0	24.0	20.5	3.7	1.54	43.6	35.0	124.5	100.2	126.7	101.9	85.6	68.9
Ba-19	[43]	7	Ax	0.1	24.0	6.0	7.0	3.8	1.48	56.2	46.3	125.0	102.9	127.4	104.9	85.9	70.7
Ba-20	[43]	9	Ax	0.1	12.0	6.0	7.0	3.7	1.56	45.2	36.2	94.9	75.9	96.7	77.3	63.5	50.8

<sup>(1)</sup>Ax=axial cyclic loading; Be=cyclic bending; <sup>(2)</sup> $T_{\sigma}=\Delta K_{I,90\%}/\Delta K_{I,10\%}$  for the N-SIF approach.

**Table 8.** Fatigue results generated by testing non-load carrying fillet cruciform welded joints (geometry Ba in Figure 1a) statistically re-analysed in terms of hot-spot stresses as well as in terms of local stress quantities.

Series	Ref.	No of Data	Load Type <sup>(1)</sup>	R	t	L	Z	k	T <sub>σ</sub> <sup>(2)</sup>	Hot-Spot Stress		Effective Notch Stress		N-SIF		TCD		
										Δσ <sub>A,50%</sub>	Δσ <sub>A,97.7%</sub>	Δσ <sub>A,50%</sub>	Δσ <sub>A,97.7%</sub>	ΔK <sub>I,50%</sub>	ΔK <sub>I,97.7%</sub>	Δσ <sub>A,50%</sub>	Δσ <sub>A,97.7%</sub>	
					[mm]	[mm]	[mm]										[MPa]	[MPa]
Bb-1	[28]	30	Be	0	4.0	4.0	4.2	4.6	1.70	91.5	70.3	171.6	131.7	175.8	134.9	118.5	91.0	
Bb-2	[28]	30	Be	0	8.0	8.0	7.7	4.1	1.98	81.1	57.6	191.8	136.2	198.3	140.8	128.4	91.2	
Bb-3	[28]	30	Be	-1	4.0	4.0	4.2	4.5	2.06	109.7	76.5	205.7	143.4	210.7	146.9	142.1	99.1	
Bb-4	[28]	30	Be	-1	8.0	8.0	7.7	5.1	1.22	119.6	108.4	224.2	203.2	287.9	260.9	194.1	175.9	
Bb-11	[39]	27	Ax	0	4.0	4.0	4.2	7.3	1.36	138.0	118.6	258.8	222.3	259.9	223.3	178.7	153.5	
Bb-12	[39]	29	Ax	0	8.0	8.0	7.7	7.0	1.62	104.6	82.0	235.7	184.9	243.5	191.1	164.3	128.9	
Bb-13	[39]	15	Ax	0	8.0	4.0	7.7	6.7	1.91	112.5	81.4	250.1	180.9	263.1	190.3	172.2	124.6	
Bb-14	[39]	28	Be	0	4.0	4.0	4.2	6.0	1.36	193.3	165.6	362.3	310.3	363.9	311.7	250.2	214.3	
Bb-15	[39]	36	Be	0	8.0	8.0	7.7	4.6	1.72	133.8	102.1	301.6	230.0	311.6	237.7	210.2	160.3	
Bb-16	[39]	27	Ax	-1	4.0	4.0	4.2	7.1	1.48	192.4	158.3	360.7	296.7	362.3	298.0	249.1	204.9	
Bb-17	[39]	9	Ax	-1	4.0	4.0	4.2	8.9	1.23	188.6	169.8	353.5	318.3	355.1	319.8	244.2	219.9	
Bb-18	[39]	34	Ax	-1	8.0	8.0	7.7	6.0	1.79	155.5	116.3	350.4	262.1	362.1	270.8	244.2	182.7	
Bb-19	[39]	21	Ax	-1	8.0	4.0	7.7	5.1	2.56	153.9	96.3	342.2	214.1	360.0	225.2	235.6	147.4	
Bb-20	[39]	30	Be	-1	4.0	4.0	4.2	5.8	1.56	238.7	190.9	447.4	357.9	449.4	359.5	309.0	247.2	
Bb-21	[39]	9	Be	-1	4.0	4.0	4.2	6.8	1.28	203.4	179.5	381.3	336.5	383.0	338.0	263.4	232.4	
Bb-22	[39]	30	Be	-1	8.0	8.0	7.7	5.3	1.51	197.1	160.5	444.2	361.8	459.0	373.9	309.6	252.2	
Bb-27	[39]	27	Ax	0	8.0	8.0	7.7	7.6	1.39	147.9	125.3	349.4	296.2	361.3	306.3	243.6	206.5	
Bb-28	[39]	18	Ax	0	8.0	4.0	7.7	7.6	1.26	160.3	142.7	356.4	317.3	364.0	324.0	245.4	218.5	
Bb-29	[39]	26	Ax	-1	8.0	8.0	7.7	5.5	4.43	188.5	89.6	445.4	211.6	460.5	218.8	310.5	147.5	
Bb-30	[39]	18	Ax	-1	8.0	4.0	7.7	6.6	1.35	225.6	194.1	501.7	431.5	512.3	440.7	345.4	297.1	
Bb-31	[44]	11	Be	0.1	10.0	10.0	7.0	3.9	1.64	60.0	46.8	137.2	107.1	99.3	77.5	65.2	50.9	
Bb-32	[44]	15	Be	0.5	10.0	10.0	7.0	3.3	1.64	55.4	43.3	126.7	99.1	91.7	71.7	60.2	47.1	
Bb-33	[45]	11	Ax	0.1	12.0	10.0	8.0	4.2	1.46	65.2	53.9	155.4	128.6	147.9	122.4	79.9	66.1	
Bb-34	[45]	13	Ax	0.1	12.0	10.0	8.0	4.0	1.38	60.4	51.4	144.1	122.7	137.2	116.8	74.0	63.0	
Bb-35	[34]	7	Ax	0.1	12.0	12.0	8.0	4.6	3.78	74.0	38.1	176.6	90.9	170.2	87.6	90.7	46.7	

<sup>(1)</sup>Ax=axial cyclic loading; Be=cyclic bending; <sup>(2)</sup>T<sub>σ</sub>=ΔK<sub>I,90%</sub>/ΔK<sub>I,10%</sub> for the N-SIF approach.

**Table 9.** Fatigue results generated by testing non-load carrying fillet welded T-joints (geometry Bb in Figure 1a) statistically re-analysed in terms of hot-spot stresses as well as in terms of local stress quantities.

Series	Ref.	No of Data	Load Type <sup>(1)</sup>	R	t	L	Z	k	T <sub>σ</sub> <sup>(2)</sup>	Hot-Spot Stress		Effective Notch Stress		N-SIF		TCD	
					[mm]	[mm]	[mm]			Δσ <sub>A,50%</sub> [MPa]	Δσ <sub>A,97.7%</sub> [MPa]	Δσ <sub>A,50%</sub> [MPa]	Δσ <sub>A,97.7%</sub> [MPa]	ΔK <sub>I,50%</sub> [MPa·mm <sup>0.326</sup> ]	ΔK <sub>I,97.7%</sub> [MPa·mm <sup>0.326</sup> ]	Δσ <sub>A,50%</sub> [MPa]	Δσ <sub>A,97.7%</sub> [MPa]
Ca-1	[28]	30	Be	0	8.0	4.0	7.7	4.0	1.67	86.7	67.1	172.3	133.5	175.7	136.1	118.5	91.8
Ca-2	[28]	30	Be	-1	8.0	4.0	7.7	3.7	1.52	100.5	81.5	199.9	162.1	203.8	165.3	137.4	111.5
Ca-3	[28]	9	Be	-1	8.0	8.0	7.7	4.0	1.59	109.6	86.9	221.3	175.4	226.2	179.2	152.7	121.0
Ca-4	[28]	10	Be	-1	8.0	4.0	7.7	2.7	2.28	107.5	71.3	213.7	141.7	218.0	144.5	147.0	97.4
Ca-9	[39]	30	Te	0	8.0	4.0	7.7	4.9	1.74	58.3	44.2	115.8	87.8	118.2	89.6	79.7	60.4
Ca-10	[39]	32	Be	0	8.0	4.0	7.7	5.3	2.01	141.8	100.0	281.9	198.9	287.5	202.8	193.9	136.8
Ca-11	[39]	31	Te	-1	8.0	4.0	7.7	4.6	2.07	87.8	61.0	174.5	121.2	178.0	123.6	120.0	83.3
Ca-12	[39]	13	Te	-1	8.0	4.0	7.7	4.6	7.61	70.9	25.7	141.1	51.1	143.9	52.2	97.0	35.2
Ca-13	[39]	12	Te	-1	8.0	4.0	7.7	3.5	4.03	108.7	54.2	219.3	109.3	224.1	111.7	151.3	75.4
Ca-14	[39]	12	Te	-1	8.0	4.0	7.7	3.9	4.57	55.5	25.9	110.3	51.6	112.5	52.6	75.8	35.5
Ca-15	[39]	27	Be	-1	8.0	4.0	7.7	5.1	1.39	170.7	144.7	339.3	287.7	346.1	293.4	233.3	197.8
Ca-16	[39]	9	Be	-1	8.0	4.0	7.7	6.3	1.75	173.2	130.8	349.5	263.9	588.7	444.4	241.1	182.0
Ca-17	[39]	9	Be	-1	8.0	4.0	7.7	7.2	1.55	175.4	140.9	348.7	280.1	355.6	285.7	239.8	192.6
Ca-18	[39]	9	Be	-1	8.0	4.0	7.7	6.6	1.49	187.2	153.6	372.2	305.4	379.6	311.5	256.0	210.0

<sup>(1)</sup>Ax=axial cyclic loading; Be=cyclic bending; <sup>(2)</sup>T<sub>σ</sub>=ΔK<sub>I,90%</sub>/ΔK<sub>I,10%</sub> for the N-SIF approach.

**Table 10.** Fatigue results generated by testing cruciform full-penetration welded joints (geometry Ca in Figure 1a) statistically re-analysed in terms of hot-spot stresses as well as in terms of local stress quantities.

Series	Ref.	No of Data	Load Type <sup>(1)</sup>	R	t	L	Z	k	T <sub>σ</sub> <sup>(2)</sup>	Hot-Spot Stress		Effective Notch Stress		N-SIF		TCD	
					[mm]	[mm]	[mm]			Δσ <sub>A,50%</sub> [MPa]	Δσ <sub>A,97.7%</sub> [MPa]	Δσ <sub>A,50%</sub> [MPa]	Δσ <sub>A,97.7%</sub> [MPa]	ΔK <sub>I,50%</sub> [MPa·mm <sup>0.326</sup> ]	ΔK <sub>I,97.7%</sub> [MPa·mm <sup>0.326</sup> ]	Δσ <sub>A,50%</sub> [MPa]	Δσ <sub>A,97.7%</sub> [MPa]
Cb-10	[39]	31	Te	0	4.0	4.0	4.2	6.0	1.84	83.1	61.3	610.3	450.2	159.7	117.8	107.6	79.4
Cb-11	[39]	23	Te	0	8.0	8.0	7.7	6.0	1.49	58.7	48.1	171.3	140.2	144.9	118.6	97.7	79.9
Cb-12	[39]	25	Te	0	8.0	8.0	7.7	5.9	1.51	50.2	40.8	146.4	119.0	123.8	100.6	83.5	67.8
Cb-13	[39]	27	Te	-1	4.0	4.0	4.2	6.5	1.76	131.8	99.2	967.8	729.0	253.2	190.7	170.7	128.6
Cb-14	[39]	11	Te	-1	4.0	8.0	4.2	5.8	2.47	155.3	98.9	555.1	353.4	279.5	177.9	188.4	119.9
Cb-15	[39]	28	Te	-1	8.0	8.0	7.7	4.4	1.98	78.3	55.6	228.5	162.3	193.2	137.3	130.3	92.5
Cb-16	[34]	12	Te	0.08	12.0	12.0	6.3	5.8	1.40	57.5	48.6	234.5	198.2	185.9	157.1	125.3	105.9
Cb-17	[34]	14	Te	0.08	12.0	12.0	6.3	4.6	1.36	53.5	45.9	218.1	187.0	172.9	148.2	116.6	99.9
Cb-19	[39]	27	Te	0	4.0	4.0	4.2	3.5	1.86	76.0	55.7	556.3	407.4	146.1	107.0	98.5	72.1
Cb-20	[39]	27	Te	0	8.0	8.0	7.7	4.2	2.14	58.6	40.0	170.7	116.6	144.3	98.6	97.3	66.5
Cb-21	[39]	18	Te	0	8.0	8.0	7.7	4.1	2.32	50.9	33.5	148.3	97.5	125.4	82.4	84.6	55.6
Cb-22	[39]	27	Te	-1	8.0	8.0	7.7	3.5	3.43	108.2	58.4	315.0	170.0	266.4	143.8	179.6	96.9
Cb-23	[42]	12	Te	0.1	12.0	12.0	8.0	5.3	2.17	45.9	31.1	206.3	140.0	136.7	92.8	92.2	62.6
Cb-24	[42]	18	Te	0.1	12.0	12.0	6.4	4.4	1.47	49.2	40.6	239.0	197.0	156.9	129.3	105.8	87.2

<sup>(1)</sup>Ax=axial cyclic loading; Be=cyclic bending; <sup>(2)</sup>T<sub>σ</sub>=ΔK<sub>I,90%</sub>/ΔK<sub>I,10%</sub> for the N-SIF approach.

**Table 11.** Fatigue results generated by testing load carrying fillet cruciform welded joints (geometry Cb in Figure 1a) statistically re-analysed in terms of hot-spot stresses as well as in terms of local stress quantities.

$\Delta\sigma_{A,50\%}^{(1)}$ [MPa]	$\Delta K_{I,50\%}^{(1)}$ [MPa·mm <sup>0.326</sup> ]	$t=L=Z$ [mm]	$\Delta\sigma_{nom,50\%}^{(1)}$ [MPa]	$L_{W-AI}$ [mm]
79.2	124.5	8	52.7	0.50
		12	46.2	0.49
		16	42.1	0.49
		20	39.1	0.48

<sup>(1)</sup>at  $2 \cdot 10^6$  cycles to failure

**Table 12.** Influence of the welded joint's absolute dimensions on the estimated value for  $L_{W-AI}$ .

n	q		
	P <sub>s</sub> =90%-10%	P <sub>s</sub> =95%-5%	P <sub>s</sub> =99%-1%
3	6.158	7.655	10.552
4	4.163	5.145	7.042
5	3.407	4.202	5.741
6	3.006	3.707	5.062
7	2.755	3.399	4.641
8	2.582	3.188	4.353
9	2.454	3.031	4.143
10	2.355	2.911	3.981
11	2.275	2.815	3.852
12	2.210	2.736	3.747
13	2.155	2.670	3.659
14	2.108	2.614	3.585
15	2.068	2.566	3.520
16	2.032	2.523	3.463
17	2.001	2.486	3.415
18	1.974	2.453	3.370
19	1.949	2.423	3.331
20	1.926	2.396	3.295
21	1.905	2.371	3.262
22	1.887	2.350	3.233
23	1.869	2.329	3.206
24	1.853	2.309	3.181
25	1.838	2.292	3.158
30	1.778	2.220	3.064
35	1.732	2.166	2.994
40	1.697	2.126	2.941
45	1.669	2.092	2.897
50	1.646	2.065	2.863

**Table A1.** Index  $q$  for a confidence level equal to 0.95% [67].

# Figures

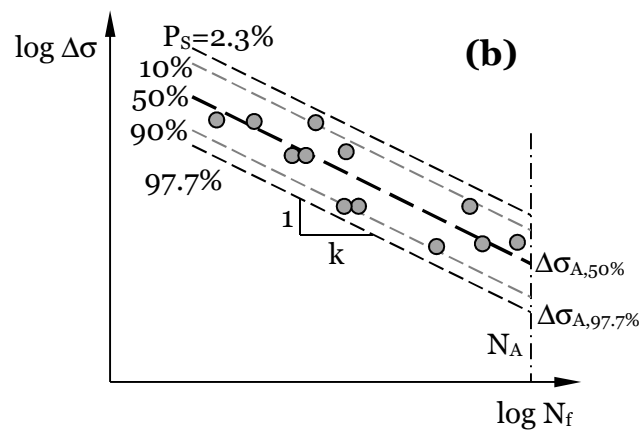
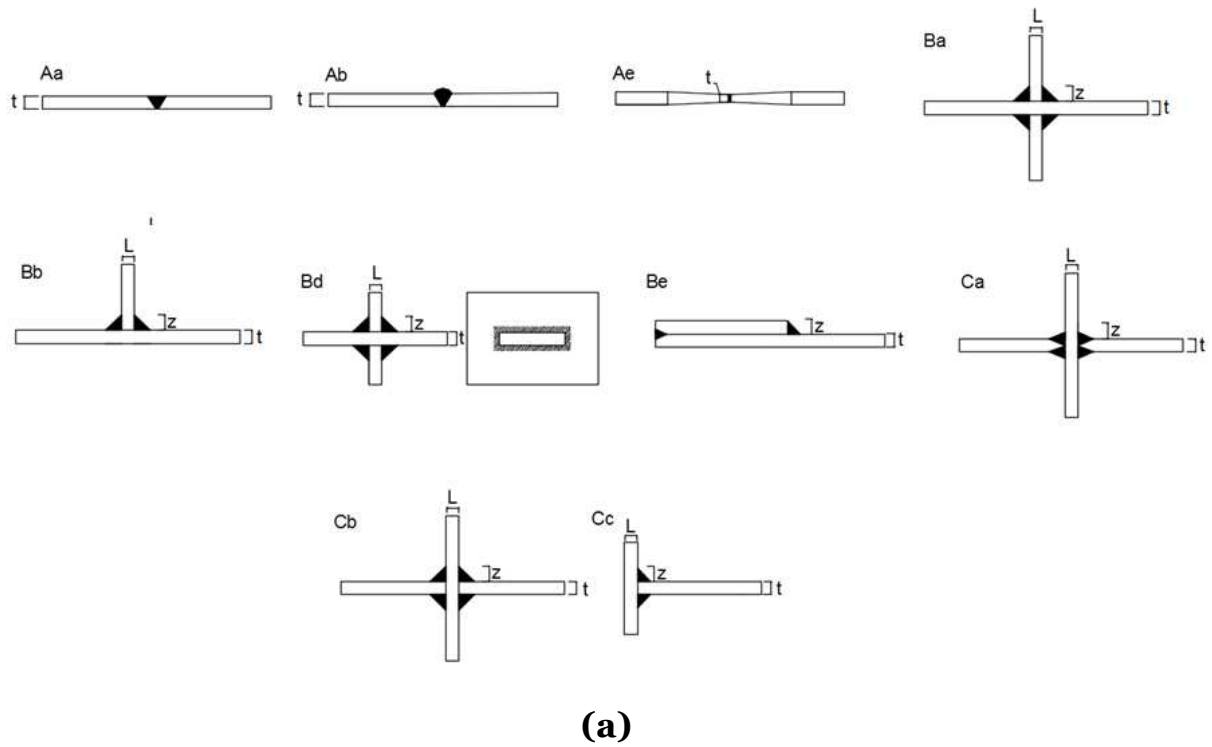


**Figure 1.** Geometry of the investigated welded details (a); Wöhler diagram (b).

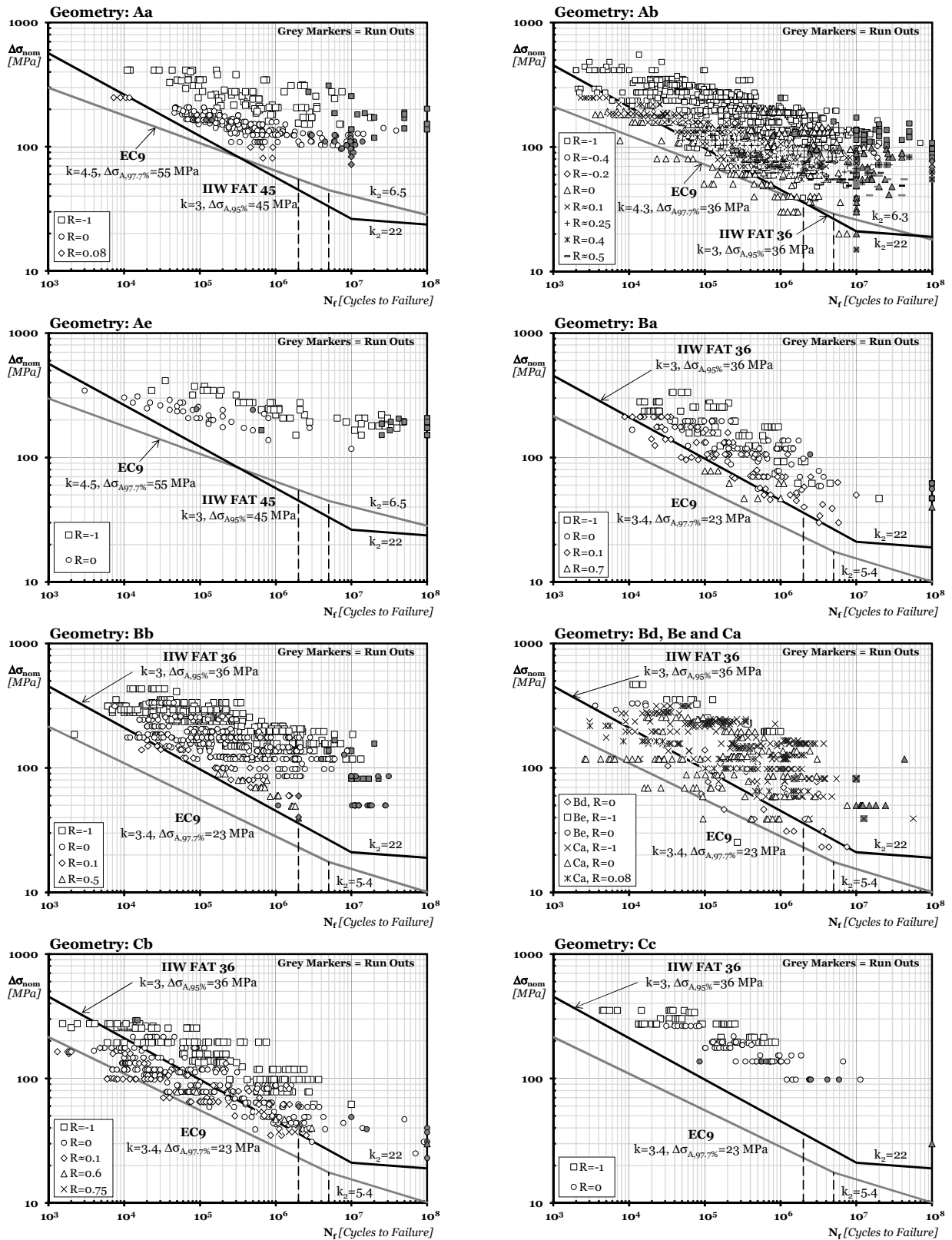
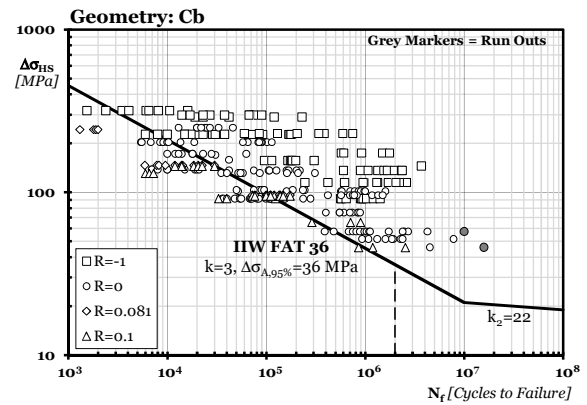
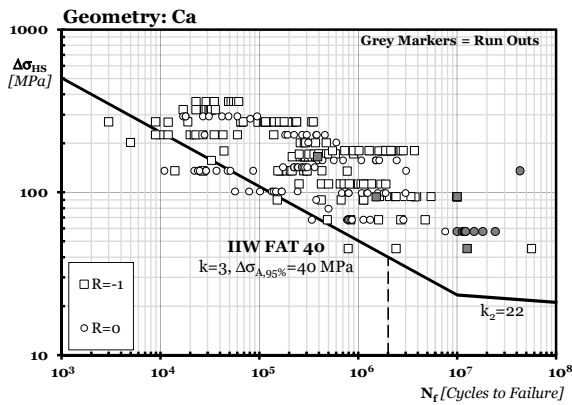
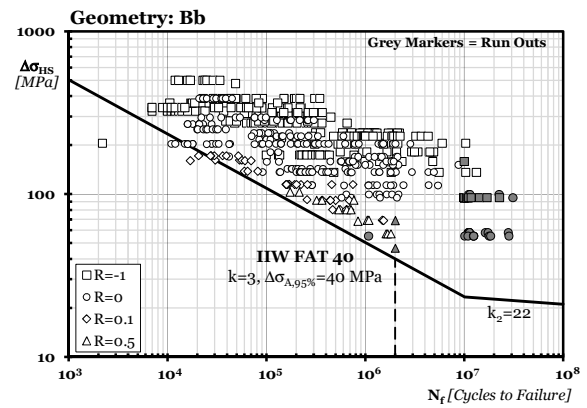
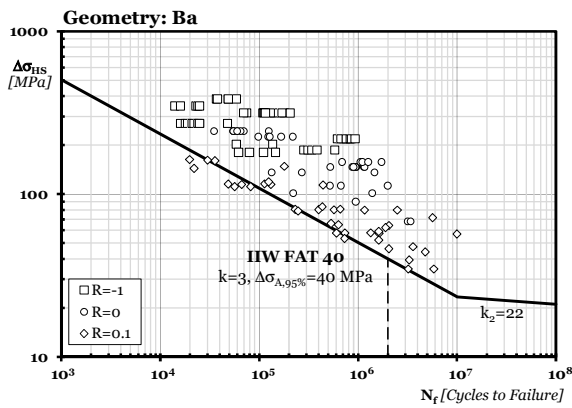
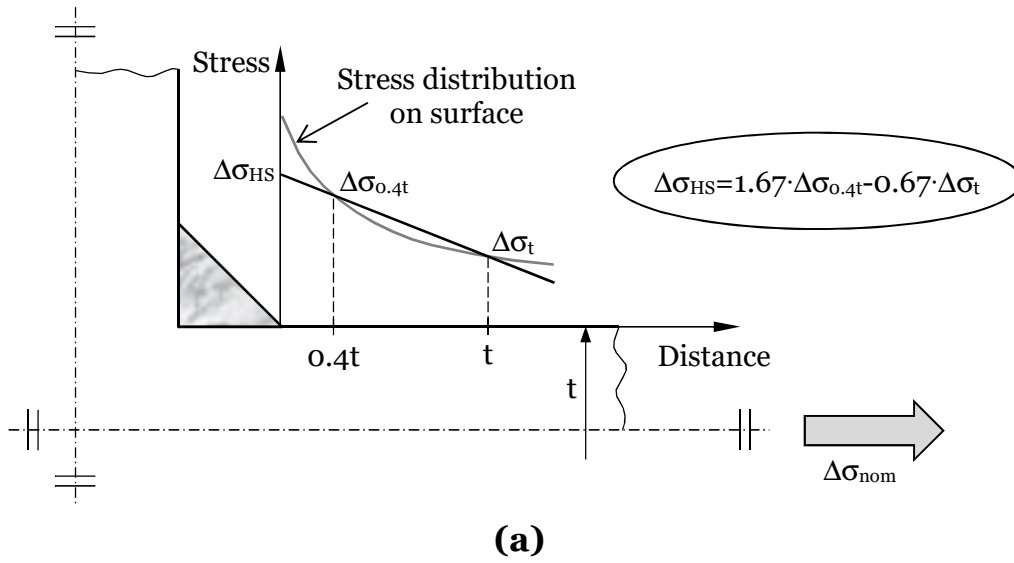


**Figure 2.** Accuracy of the Nominal Stress approach in estimating the fatigue strength of the investigated welded joints - see Fig. 1a for the definition of the different welded geometries.



(b)

**Figure 3.** Definition of hot-spot stress (a); accuracy of the Hot-Spot Stress approach in estimating the fatigue strength of the investigated welded joints (b) - see Fig. 1a for the definition of the different welded geometries.

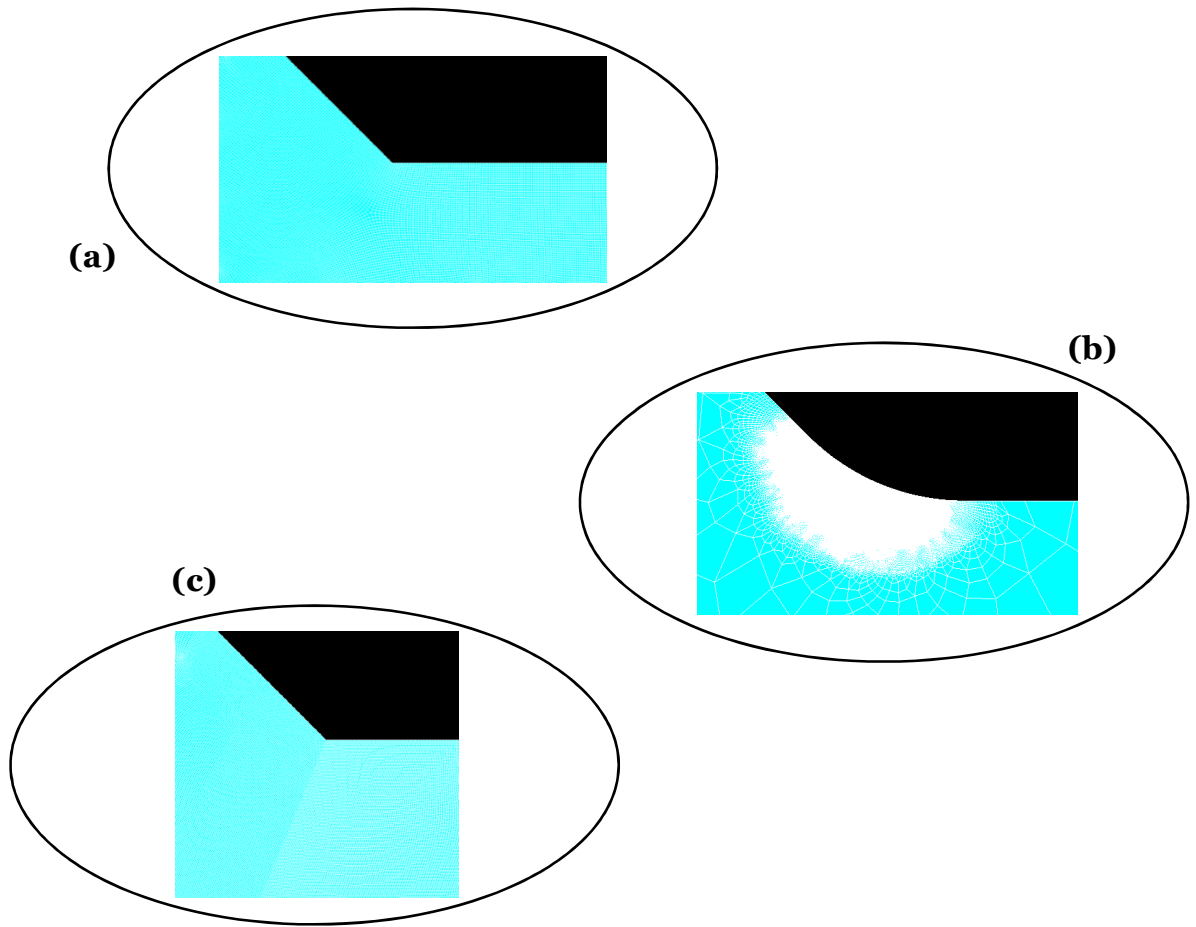
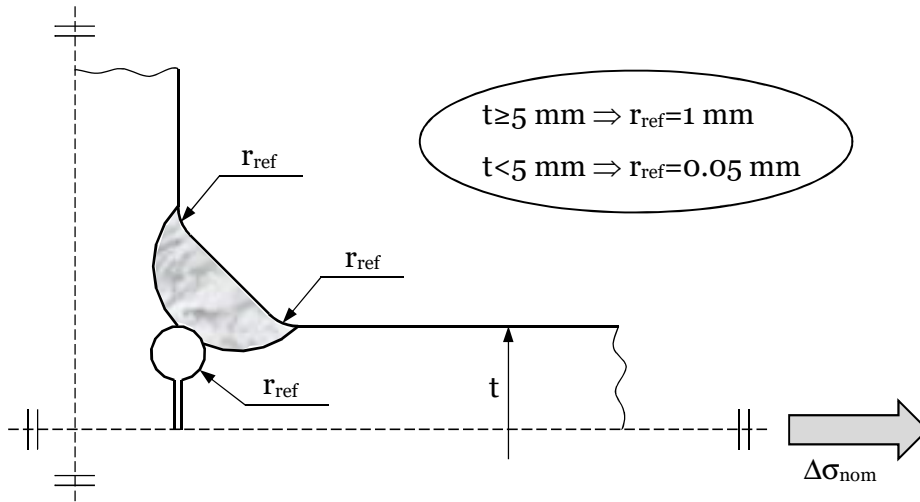
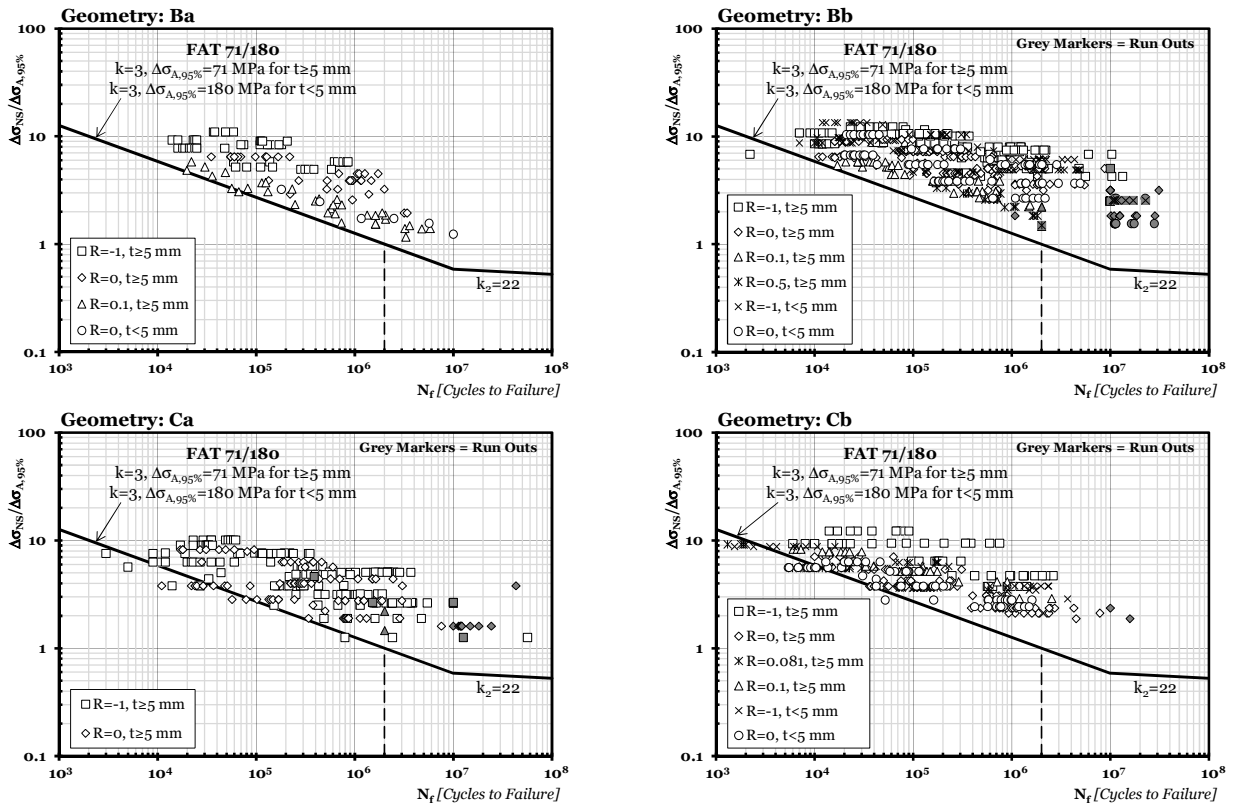


**Figure 4.** *Examples of FE models being solved.*

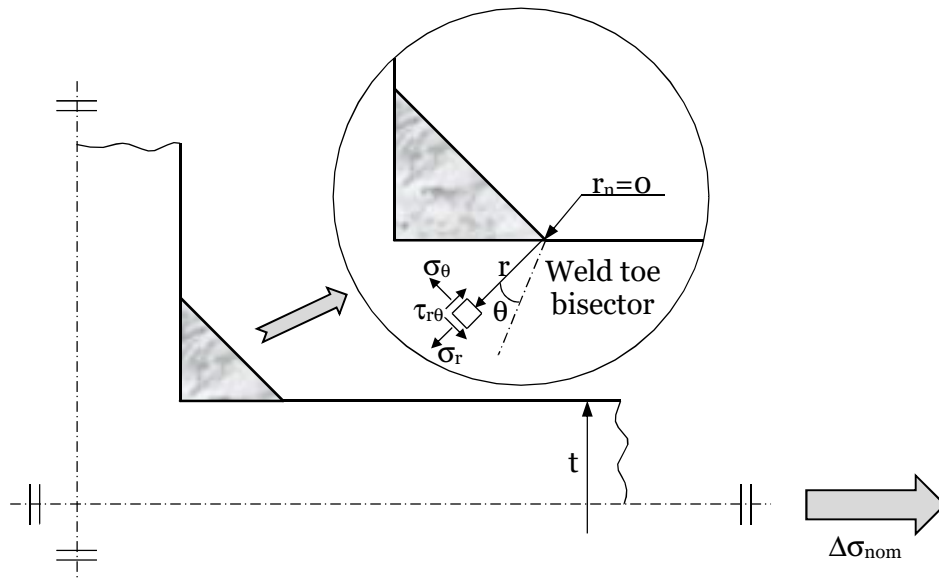


(a)

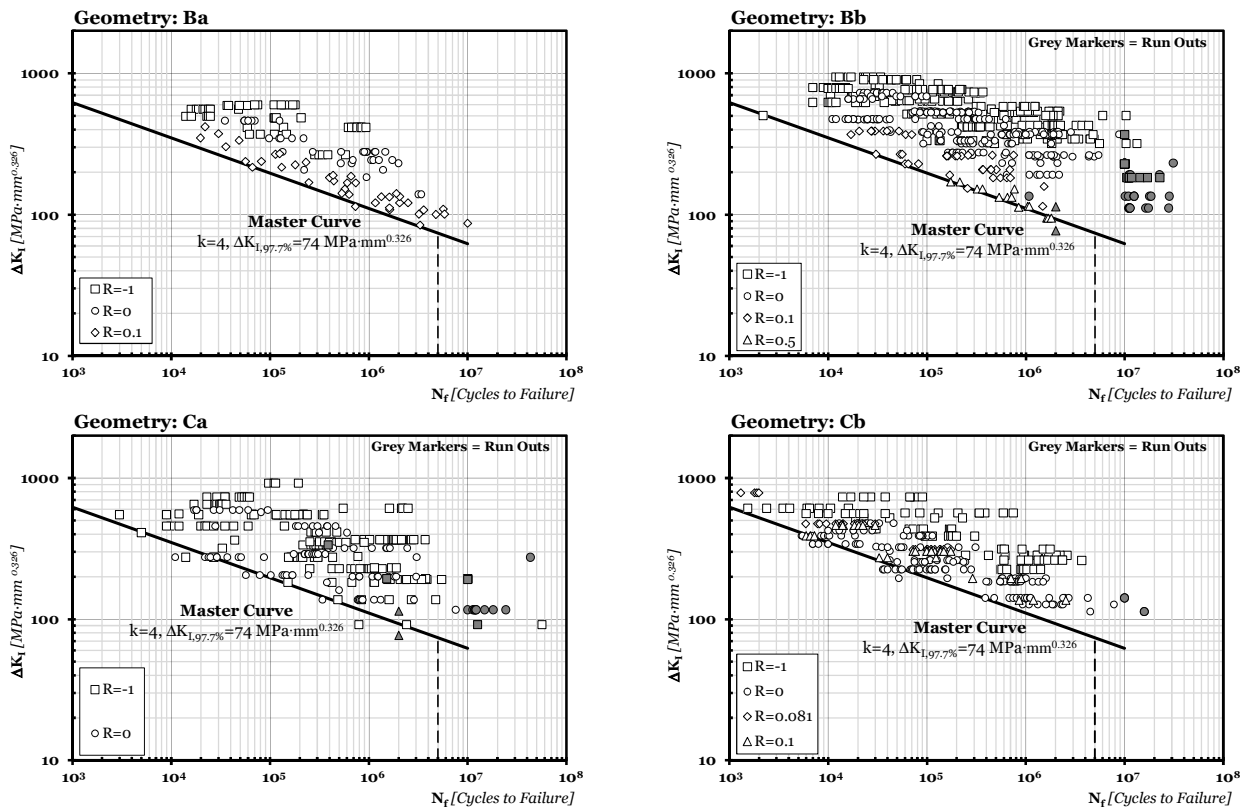


(b)

**Figure 5.** Weld toe and root rounded according to the reference radius concept (a); accuracy of the Effective Notch Stress approach in estimating the fatigue strength of the investigated welded joints (b) - see Fig. 1a for the definition of the different welded geometries.

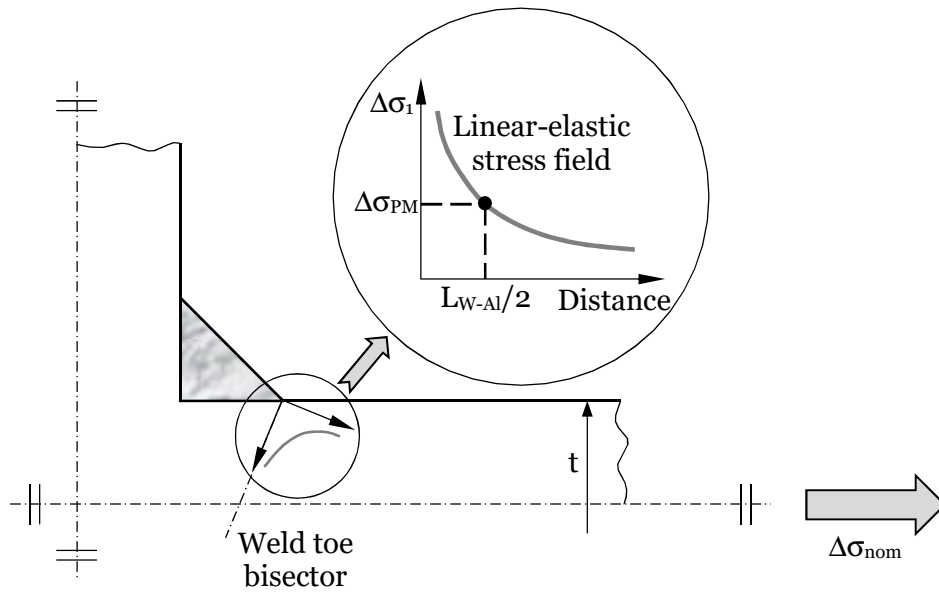


(a)

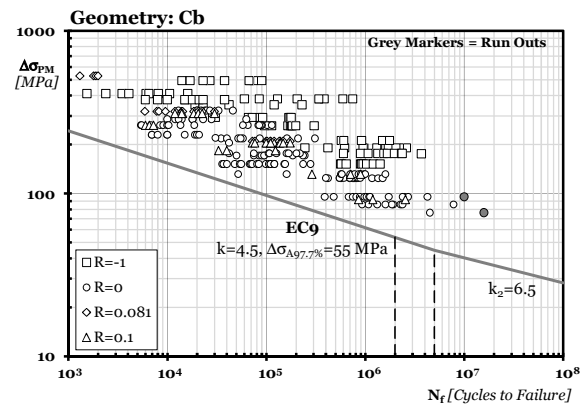
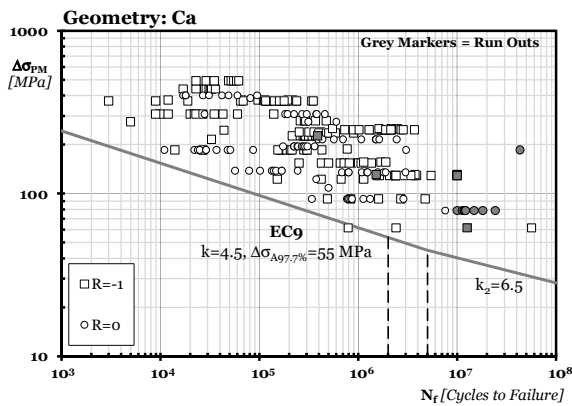
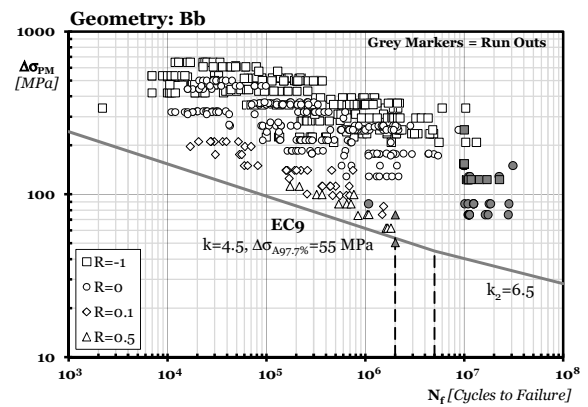
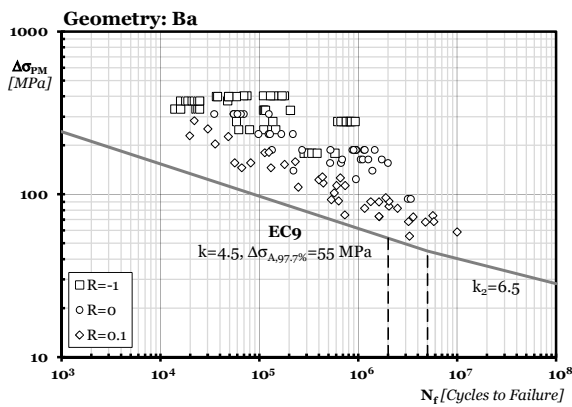


(b)

**Figure 6.** Local stress state in the vicinity of the weld toe (a); accuracy of the  $N$ -SIF approach in estimating the fatigue strength of the investigated welded joints (b) - see Fig. 1a for the definition of the different welded geometries.

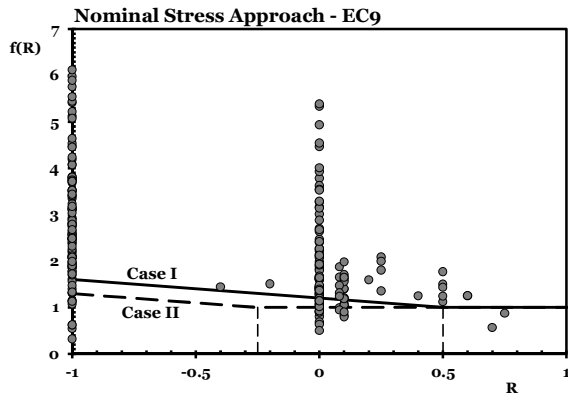


(a)

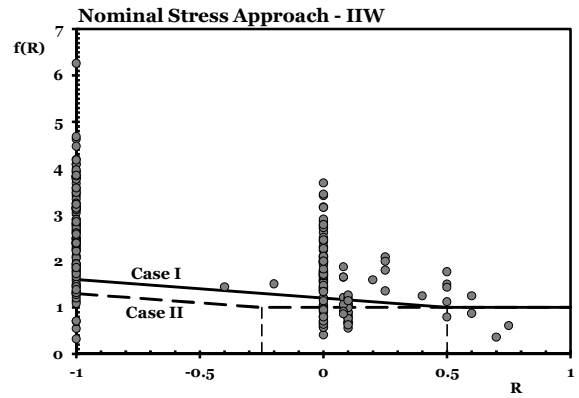


(b)

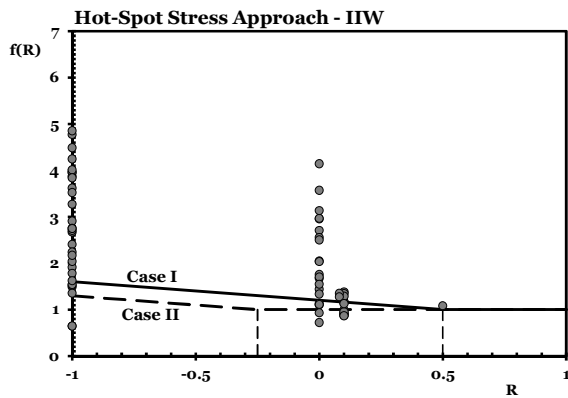
**Figure 7.** Local stress-distance curve and critical distance  $L_{W-AI}$  according to the PM (a); accuracy of the PM in estimating the fatigue strength of the investigated welded joints (b) - see Fig. 1a for the definition of the different welded geometries.



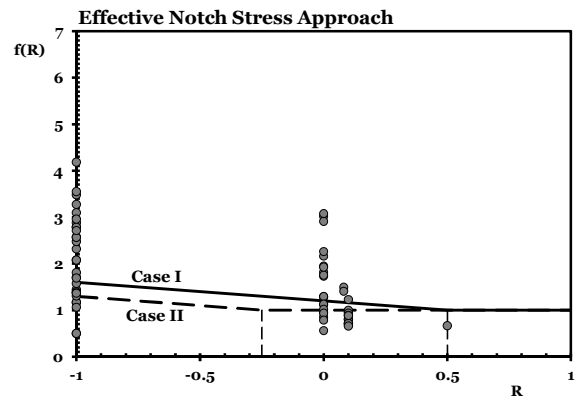
(a)



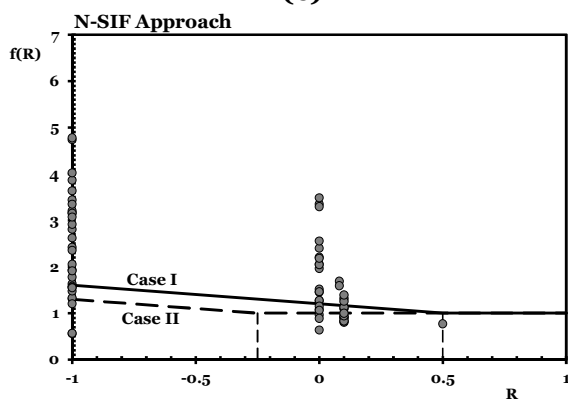
(b)



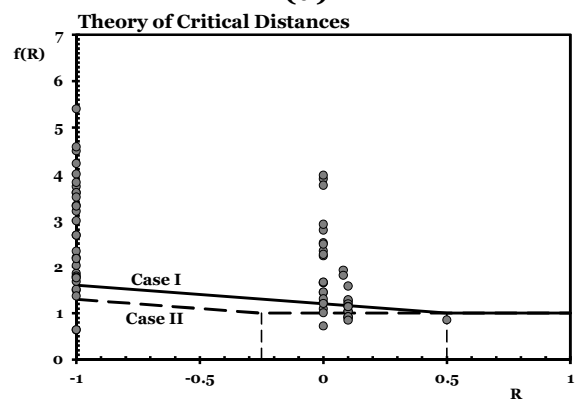
(c)



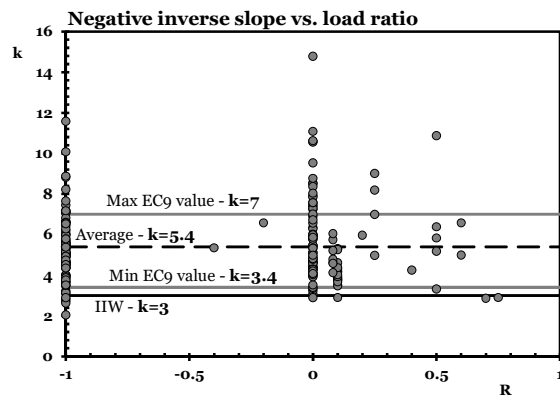
(d)



(e)



(f)



(g)

**Figure 8.** Effect of load ratio  $R$  on the fatigue strength of aluminium welded joints.

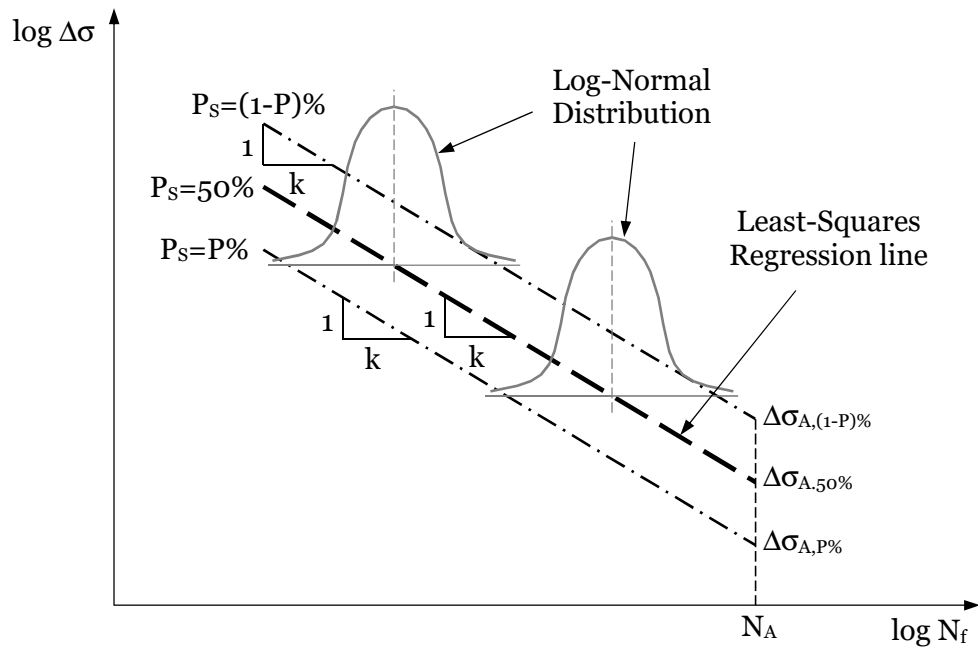


**Figure A1.** Wöhler diagram showing fatigue curves calculated for different probabilities of survival.